UV-LED IRRADIATION TECHNOLOGY FOR POINT-OF-USE WATER DISINFECTION IN DEVELOPING COMMUNITIES

By

CHRISTIE CHATTERLEY

B.S., Idaho State University, 2003

A thesis submitted to the Faculty of the Graduate School of the
University of Colorado at Boulder
in partial fulfillment of the requirements for the degree of
Master of Science
Department of Civil, Environmental, and Architectural Engineering
2009

ProQuest LLC
789 East Eisenhower Parkway
P.O. Box 1346
Ann Arbor, MI 48106-1346

This thesis entitled:

UV-LED Irradiation Technology for Point-of-Use Water Disinfection
in Developing Communities

written by Christie Chatterley

has been approved for the Department of Civil, Environmental,
and Architectural Engineering

Karl G. Linden

Kevin McCabe

Fernando Rosario-Ortiz

Date: _____

The final copy of this thesis has been examined by the signatories, and we find that both the content and the form meet acceptable presentation standards of scholarly work in the above mentioned discipline.

Chatterley, Christie Anne (M.S., Civil Engineering [Department of Civil, Environmental, and Architectural Engineering])

UV-LED Irradiation Technology for Point-of-Use Water Disinfection in Developing Communities

Thesis directed by Professor Karl G. Linden

Abstract

Ultraviolet (UV) irradiation is a common disinfection option for water treatment in the developed world. There are a few systems installed in developing countries for point-of-use treatment, but the low-pressure mercury lamps currently used as the UV irradiation source, have a number of sustainability issues including a short lifetime of approximately one year and toxic mercury inside that must be disposed of after they are used. UV light emitting diodes (LEDs) may present solutions to many of the sustainability issues presented by current UV systems. LEDs are small, efficient, have long lifetimes, and do not contain mercury. LEDs have recently become available in the germicidal wavelength range and this research assessed their efficiency for inactivation of *E. coli* in water compared to low-pressure lamps. A UV-LED prototype was also evaluated as a proof-of-concept of this technology for a point-of-use disinfection option.

Acknowledgments

I would like to thank my advisor Dr. Karl G. Linden in the Civil, Environmental and Architectural Engineering (CEAE) Department for his support and guidance throughout this project. I am also greatly appreciative of Dr. Kevin McCabe, a research associate in the department of Civil, Environmental and Architectural Engineering for his mentorship on the microbiological aspects of this research. This work was funded by a fellowship from the National Water Research Institute (NWRI) and a grant from the University of Colorado Engineering Excellence Fund (EEF). I am also grateful to Tim Bettles of Crystal IS, a UV-LED manufacturing company for his help understanding the science behind UV-LEDs and expressing his company's expectations for future costs and lifetimes of UV-LEDs. Tim May from the University of Colorado Integrated Teaching and Learning Laboratory (ITLL) was also extremely helpful during the building of the electrical circuits to power the LEDs. I would also like to thank Naomi Levine, a student at a local high school, and Christina Barstow who helped with lab experiments. David Sparkman and professor Jeffrey T. Luftig, (aka. the Stats Master) were incredibly helpful with the statistical analysis. . I also want to thank Hadas Mamane-Gravetz who helped me fit my data to her model while she was in Israel. I owe a great deal of thanks to Kate Kowalski for her help getting started in the lab, Aaron Dotson for his help acquiring materials, Chris Corwin for his advice in lab procedures, and all the students in Dr. Scott Summer's and Dr. Karl Linden's lab groups. And, of course, I owe a huge amount of gratitude to all of my friends and family who have supported me before and throughout this research.

Table of Contents

Table of Tables

Table of Figures

1. Research Objectives

The objective of this project is to evaluate the efficacy of Ultraviolet Light Emitting Diode (UV-LED) technology for the development of point-of-use (POU) water disinfection systems to improve public health in rural communities in a sustainable, environmentally responsible manner. There are a number of POU technologies available, but the application of UV-LEDs as a disinfection source will provide an additional technology to the POU toolbox that will enable longer-life disinfection systems with low user input and very low energy cost compared to current low-pressure mercury lamps. This will improve public health by increasing system reliability and decreasing maintenance needs.

Specifically, this research seeks to evaluate the use of UV-LEDs at 265 nm for inactivation of *E. coli* in water through meeting the following objectives:

- Determine if UV-LEDs at 265 nm are more efficient than low-pressure lamps (254 nm) for inactivation of *E. coli* (based on the action spectra of *E. coli* (Figure 0))
- Build and evaluate a point-of-use UV-LED prototype
- Determine if UV-LEDs are a feasible option for water treatment

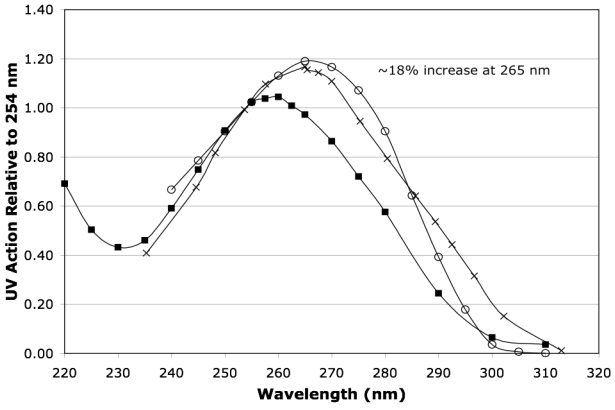

Figure 0. Action Spectra for DNA (■) and *E. coli*. DIN Standard (○) and ISE Standard (×)

2. Introduction

2.1 The Need for Point-of-Use Treatment Options

Diarrheal illnesses are one of the leading causes of morbidity and mortality in developing countries (Pruss et al., 2002, WHO, 2002). In many analyses of interventions to reduce diarrhea, "improved water quality" is shown to have a lower effect than other interventions such as sanitation and hygiene. However, these reviews focus upon *source* water quality improvements rather than improvements at *point-of-use* (Gundry et al, 2004). Fewtrell and Colford (2004), showed the increased impact of treating water at the household level compared to treating at the source. This information has created an interest in household water treatment technologies. A number of point-of-use technologies have been evaluated including boiling, biosand filtration, chlorination, chlorination plus flocculation, solar disinfection (SODIS), and ceramic filters (Sobsey et al., 2008). Disinfection using ultraviolet (UV) radiation in the UV-C range may be a more favorable option for many applications. It does not utilize chemicals and disinfects at much higher rates than SODIS which utilizes radiation in the UV-A range.

UV disinfection is a well-established disinfection technology that has been used in centralized water and wastewater facilities in developed countries for decades. UV radiation inactivates bacteria, viruses, and protozoa, with the benefits of no taste and odor issues, no known disinfection byproducts (DBPs), no danger of overdosing, relatively fast treatment rates compared to sand and ceramic filters, and low-maintenance. Over the last ten years, small UV systems have become available, including commercially available systems such as Sterilight and the low-cost, locally

manufactured UV-Tube system that have become an appropriate treatment option for developing communities in a number of countries including Mexico, Rwanda, Sri Lanka, and India (Reygadas et al., 2006).

2.2 Benefits of UV-LEDs

UV disinfection can be an improvement over other treatment options, such as chemical disinfection, for many applications, but there are sustainability issues that arise from current low-pressure lamp systems. They use toxic mercury as the UV radiation source and typically only last for around one year (8,000-10,000 hours) at which time communities are faced with a number of issues: finding and paying for replacement lamps, transporting these fragile glass and filament tubes, and disposing of mercury contained in the used lamp in areas that do not always have a toxic waste disposal system (US EPA, 2006).

UV light emitting diodes (LEDs) may provide solutions to many of the sustainability issues of UV mercury lamps. They are small (5-9 mm diameter), and do not contain glass, filament or mercury, aiding their transport and disposal (Bettles et al., 2007). Warm-up time is not required for LEDs, saving energy and allowing for intermittent use and quick recovery from a power failure—important characteristics for rural applications especially. LEDs are replacing a number of light sources currently utilized today including traffic lights and household lights. LEDs have an excellent track record for lowering system costs through energy savings, lower maintenance, and longer replacement intervals. The average electrical-to-germicidal efficiency of low-pressure UV mercury tube lamps is 35-38% (US EPA, 2006).

Visible LEDs can operate at 75% efficiency for ten years (100,000 hours) (Bettles et al., 2007). Currently, the efficiencies of UV-LEDs are less than 1% with lifetimes of around 1,000 hours (Bettles et al., 2007; Gaska, 2007). Although research of this technology is still in its infancy, improvements to UV-LEDs are expected to occur rapidly following visible LED source trajectories, resulting in a high efficiency, low power input.

Another benefit of UV-LEDs is their wide range of operating temperatures, which may allow them to be utilized in locations with extreme temperatures, particularly cold temperatures since the power output increases at lower temperatures. At 5°C, the UV-LEDs from SET, produce about 35% more power compared to room temperature (SET UV-TOP Technical Data, 2008). Low-pressure mercury lamps run at optimal level at room temperature and the efficiency will rapidly decrease at temperatures on either side of this (Crawford et al., 2005).

Temperature has been thought to have a large effect on thymine dimer formation, with an increased rate of thymine dimer formation at temperatures less than 25°C due to the stacked configuration of DNA at lower temperatures that is more subject to dimerization (Rahn, 1970). In regions of cold temperatures, this increase in disinfection efficiency could be taken advantage of with UV-LEDs. However, recent studies have shown there is little to no change in dimer formation at temperatures of 5, 20, and 35°C (Severin et al., 1983).

The availability of specific output wavelengths using UV-LEDs may also increase their inactivation efficacy. UV-LEDs currently operate in the wavelength range of 247-365 nm (Gaska, 2007). Effective UV sources should emit high

intensities in the peak absorbance wavelengths of DNA—the germicidal target of UV photons. However, germicidal effectiveness as a function of wavelength can vary for different microorganisms and may differ from the DNA absorbance spectrum, as illustrated in **Error! Reference source not found.**.

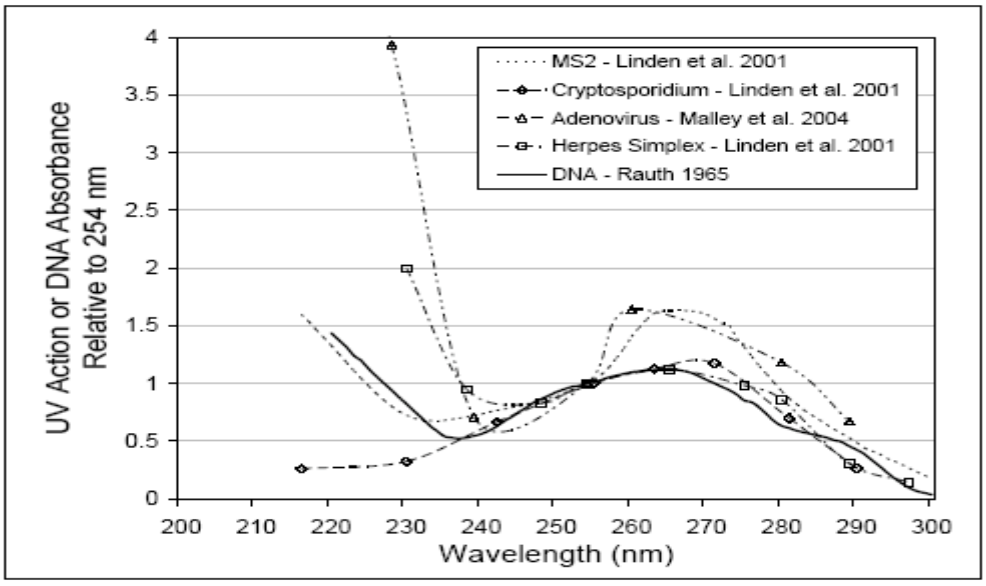

Source: Adapted from Rauth (1965), Linden et al. (2001), and Malley et al. (2004)

Figure 2. UV germicidal effectiveness for various microorganisms (US EPA, 2006)

Supplementing peak DNA wavelengths with other UV emissions may provide a synergistic disinfection effect, increasing the effectiveness of UV inactivation of pathogens (US EPA, 2006; Mamane-Gravetz et al., 2005). Low-pressure lamps are monochromatic (254 nm) and some pathogens, such as adenovirus, are not most effectively inactivated at this wavelength. Mamane-Gravetz et al., 2005, found that MS2 bacteriophage was three times more sensitive to wavelengths around 214 nm compared to 254 nm and *B. subtilis* spores were more effectively inactivated around 265 nm. Medium Pressure lamps are polychromatic, but peak intensities occur at set

wavelengths based on the emission properties of mercury. A distinct advantage over conventional UV sources is that UV-LED systems can incorporate an LED array of differing wavelengths, maximizing their combined germicidal effect. This would allow units to be custom designed based on the specific microbial contaminants of source waters, or for a broad range of pathogens under a single system.

2.3 Greater Good/Ramifications

Many rural systems in the United States and in less developed communities rely on minimally experienced operators. This technology could decrease operator involvement while increasing system reliability and providing long-term operation. Other benefits include less mercury released to the environment, a safer, lower maintenance option than chlorination and sand filtration, and less waste due to the longer lifetime of LEDs.

In San Andres, Guatemala, there is running, low-turbidity, water in the local homes. However, families need to purchase five gallon plastic bottles of potable water for drinking needs. A small, point-of-use, UV-LED disinfection unit could reduce household drinking water expenses and improve community public health while reducing the need for these plastic bottles.

In 2007, Engineers Without Borders at the University of Colorado designed and implemented six rainwater catchment systems at an orphanage in Mugonero, Rwanda. These systems will provide water for cooking, cleaning, and bathing, but will not be drinking water quality. The water will still need to be boiled for drinking water needs since the residence do not like the taste of chlorine, a very costly process in a country where wood is extremely scarce. A small, photovoltaic powered UV-

LED system attached to the orphanage-based rainwater storage tanks could alleviate both time consuming trips to the community tap forty minutes away and reduce orphanage costs for fuel wood, as well as promote clean water consumption and public health.

3. Background

3.1 Fundamentals of Photochemistry

3.1.1 Characteristics of Ultraviolet Light

Ultraviolet Light is characterized by light in the wavelengths of 100-400 nm, including vacuum UV (100 to 200 nm), UVC (200 to 280 nm), UVB (280 to 315 nm), and UVA (315 to 400 nm) (ISO 21348, 2007). Vacuum UV is a very effective disinfectant, but is quickly absorbed by most substances and impractical for water treatment. UVC is a higher energy than UVA and UVB and is the main source of germicidal action in current UV disinfection systems.

The energy emitted by light can be calculated using Planck's Law of Radiation:

$$u = h\nu = hc/\mu$$

where u is the energy of one photon (J), ν is the frequency (s^{-1}), λ is the wavelength (m), c is the speed of light in a vacuum (3.0×10^8 m/s), and h is the Planck constant (6.626×10^{34} J s).

3.1.2 Terms and Concepts (Bolton, 2000; Verhoeven, 1996)

Source Radiant Power (Φ): The total radiant power emitted in all directions by a radiant energy source (units, W).

Source Radiant Energy (Q): The total radiant energy emitted from a source over a given period of time (units, J).

Irradiance (E): The total radiant power from all upward directions incident on an infinitesimal surface element with area dS containing the point under consideration divided by dS (units, mW/cm^2).

Fluence Rate (E'): The total radiant power incident from all directions onto an infinitesimally small sphere with cross-sectional area dA, divided by dA (units, mW/cm^2).

UV Dose or Fluence (H'): The total radiant energy from all directions passing through an infinitesimally small sphere of cross-sectional area dA, divided by dA (units, mJ/cm^2). Equals the Fluence Rate (mW/cm^2) multiplied by the irradiation time in seconds.

3.1.3 Absorbance and Transmittance: The Beer-Lambert Law

UV light will be attenuated by any substance that is capable of absorbing it. The ability of a substance to absorb light is calculated using the Beer-Lambert Law and quantified as absorbance or transmittance.

Absorbance (A) is a unitless value used to quantify the decrease in incident light as it passes through a water sample over a specified distance (path length); i.e. how much light was absorbed. It can be calculated using the Beer-Lambert Law by:

$$A = \log\left(\frac{I_o}{I}\right),$$

where A is the absorbance at a specified wavelength and path length, I_o is the intensity of light incident on the sample (mW/cm^2), and I is the intensity of light transmitted through the sample (mW/cm^2).

UV Transmittance (UVT) refers to the percentage of light passing through a medium over a specified distance, calculated by the Beer-Lambert Law by:

$$UVT\,(\%) = 100 \times \frac{I}{I_o},$$

where UVT is the UV transmittance at a specific wavelength and path length, I is the intensity of light transmitted through the sample (mW/cm^2), and I_o is the intensity of light incident on the sample (mW/cm^2).

Transmittance and Absorbance are related by:

$$UVT\,(\%) = 100 \times 10^{-A}$$

or

$$A = -\log\left(\frac{UVT(\%)}{100}\right)$$

If the attenuation of light is mainly due to absorption, transmittance can also be calculated by:

$$UVT\,(\%) = 10^{-\alpha l},$$

where α is the absorption coefficient at a specified wavelength (cm^{-1}), and l is the path length (cm).

The absorption coefficient (α) is related to the absorbance (A) at a specified wavelength by:

$$\alpha = \left(\frac{A}{l}\right)\ln(10)$$

4. Literature Review

Limited research has been conducted on the effectiveness of UV-LEDs for water disinfection. Most of the data available are for LEDs that output light in the UVA range (320-400 nm), which is less efficient at disinfection than light in the germicidal range of UVC (200-280 nm) since it is poorly absorbed by DNA (Sinha and Häder, 2002; ISO 21348, 2007). UVA radiation inactivates microorganisms by damaging proteins and producing hydroxyl and oxygen radicals that can destroy cell membranes and other cellular components (Sinha and Häder, 2002). This process takes more time than the damage produced by UV-C, which directly effects the DNA of microorganisms by producing cyclobutane thymine dimers, 6-4 photoproducts, and spore photoproducts (if spores are present), inactivating them without intermediate steps (Grossweiner and Smith, 1989).

Hamamoto, et al., 2007, demonstrated the ability of UVA-LEDs at 365 nm to inactivate bacteria in water. They found that *E. coli* DH5α were reduced by >5 log at a dose of 315 J/cm^2 (Hamamoto et al., 2007). UVA is poorly absorbed by DNA, but can damage proteins and produce hydroxyl and oxygen radicals that can destroy cell membranes and other cellular components (Sinha and Häder, 2002). This process takes more time than the damage produced by UVC, which directly effects the DNA of microorganisms by producing cyclobutane thymine dimers, 6-4 photoproducts, and spore photoproducts (if spores or dehydrated vegetative cells are present), inactivating them without intermediate steps (Grossweiner and Smith, 1989).

Sandia National Laboratories documented inactivation of E. coli with UVC-LEDs at 270 nm (Crawford et al., 2005). Two strains of E. coli, ATCC #23229 and

#15596, shown to have a high and medium sensitivity to UV respectively, were evaluated. Tests were conducted while the *E. coli* were in early log growth phase and were centrifuged for one hour and suspended in phosphate buffer solution (PBS). This process was repeated twice resulting in an initial *E. coli* concentration of 10^5 and absorbance values of 0.0136 and 0.0234 for ATCC #15597 and #23229, respectively. Results for E. coli #15596 show an increased inactivation efficiency compared to the Environmental Protection Agency (EPA) inactivation data for 254 nm low-pressure (LP) sources: 1.85 log reduction with a dose of 2.2 mJ/cm^2 for the LEDs, compared to a 2 log reduction with a dose of 6 mJ/cm^2 utilizing a LP lamp (Crawford et al., 2005). Results were inconclusive for E. coli #23229 due to inconsistencies in the data.

Sensor Electronics Technologies (SET) have demonstrated inactivation of *E. coli* B (ATCC #11303) using 265-310 nm UV-LEDs (Gaska, 2007). SET reports that inactivation was highly wavelength dependent with inactivation decreasing by more than six orders of magnitude for the 310 nm LEDs compared to the 265 nm LEDs. They also report that the killing efficiency of the UV-LEDs exceeded that of LP lamps, but neither methods nor data were reported (Gaska, 2007).

5. Materials and Methods

5.1 Test Configurations

5.1.1 Low-Pressure Testing

Testing of low-pressure (LP) lamps was performed using a UV collimated beam apparatus consisting of three LP mercury lamps housed inside a wooden enclosure with a circular aperture at the bottom for the light to exit and irradiate the sample below. The inside of the wood box was painted black and a piece of cardboard was used as a shutter to cover the aperture between exposures. The UV lamps were turned on ten minutes prior to the irradiation of samples based on the measured warm-up time.

5.1.2 Set-up for UV-LED Batch System

An array of three UV-LEDs was created using a circuit wire-wrapped, with 30 gauge wire, to an electronic Perfboard (a fiberglass board with holes every $1/10^{th}$ inch). A 150-ohm resistor was wired in series with each LED to create 6 volts across each LED at 20 amps with a 9 volt input voltage from a power supply. These values are within manufacturer specifications for voltage and current. Socket pins were wire-wrapped to the Perfboard to hold the LEDs in place for easy removal and replacement.

5.1.3 Set-up for UV-LED Flow-Through Prototype

A row of ten UV-LEDs was created using a circuit wire-wrapped, with 30 gauge wire, to an electronic Perfboard. A 150-ohm resistor was wired in series with

each LED to create 6 volts across each LED at 20 amps with a 9 volt input voltage from a power supply. The LEDs were placed over a ¼" x ¼" aluminum trough and water was pumped through the trough below the LEDs.

5.2 Irradiance Measurement

5.2.1 Radiometer Measurement

Irradiance was measured with a radiometer (International Light IL1400A) calibrated at 254 nm. The response curve in Figure 3 was used to convert the radiometer reading to the output wavelength of the LEDs. For example, for 265 nm, the reading was decreased by 17.3%.

Figure 3. Microbial Response Curve for IL1400 Radiometer

The irradiance over time (0, 1, 2, 5, 10, and 20 minutes) was measured to determine the warm-up time of both the low-pressure (LP) lamps and the UV-LEDs. Irradiance of an array of one 265 nm hemispherical lens UV-LEDs was measured at five distances from the source, up to five cm, to estimate the effect of distance on irradiance changes, specifically for modeling and estimating dose predictions for the prototype unit.

5.2.2 Spectrometer Measurement

The absolute irradiance and spectral output of each LED was tested, using an Ocean Optics spectrometer 1 mm from the source. The LEDs tested included four flat top 265 nm lamps, one flat top 250 nm lamp, one flat top 280 nm lamp, and one hemispherical lens 280 nm lamp.

5.2.3 Actinometry

Chemical actinometry was used to evaluate the irradiance values measured by the radiometer for the LP lamps and LEDs. Actinometry uses a chemical with a known UV decay to measure the UV dose. For this research, the potassium iodide/iodate (KI/KIO_3) actinometer was used based on the method found in Rahn et al. 2003. The actinometer solution was made up of 0.6 M KI, 0.1 M KIO_3, 0.01 M $Na_2B_4O_7$ in 100 mL of deionized water that was rapidly mixed on a stir plate until completely dissolved. The absorbance of the solution was recorded for 300 nm and 352 nm. Samples of the solution were irradiated and the absorbance was recorded for each irradiated sample at 352 nm. Irradiation times were based on an irradiated sample absorbance at 352 nm of less than 1.4 since absorbance data becomes more

unreliable above 1. Detailed calculations and instructions can be found in Appendix A based on the method used by Bolton Photosciences Inc. The quantum yield (Φ) used for the low pressure test (254 nm) was 0.73 (Rahn et al. 2003). For the UV-LED batch system test (265 nm), a quantum yield of 0.57 was used based on a linear relationship between wavelength and quantum yield between 254 nm (Φ = 0.73) and 284 nm (Φ = 0.3) (Rahn et al. 2003). Details can be found in Appendix A.

The LP system was tested at a lamp to detector/water surface distance, L, of 40.2 cm and the UV-LED batch system was tested at an L of 0.6 cm. The distance for the UV-LED batch system needed to be much closer due to the low intensity of the three LEDs compared to the lamps used in the LP system.

5.3 Microbial Testing

E. coli was used as an indicator organism to compare the efficiency of the LP and UV-LED systems, and to evaluate the UV-LED prototype. The dose response was evaluated for three *E. coli* strains at log growth phase and stationary phase irradiated by LP lamps and UV-LEDs. Growth curves were developed to identity log growth phase. Samples were irradiated using a low-pressure quasi-collimated beam apparatus and a UV-LED batch system and log-inactivation information was compared.

5.3.1 Bacteria Strains

The first *E. coli* strain used in these experiments was obtained from Kate Kowalski, a previous graduate student at the University of Colorado. It is believed to be *E. coli* K12, but it is not certain. Purity was verified by streak plating and visual

observation on tryptic soy agar (TSA, Difco #236950). An antibiotic resistant *E. coli* strain DH5α [*endA1 hsdR17 supE44 thi-I recA1 gyrA relA1 Δ(lacIZYA-argF)U169 ϕ*80 *Δlac-ZM15*] was obtained from Kevin McCabe, a research associate in the CEAE department. Details of the strain can be found in Chao et al., 2002. *E. coli* K12 was obtained directly from ATCC (#29425).

5.3.2 Preparation of Inoculum

For testing in the stationary phase, colonies were obtained from TSA plates after overnight incubation at 37°C using sterile methods and added to a 500 mL glass bottle of sterile tryptic soy broth (TSB, Cellgro #61-412-RO). This stock solution was place in the 37°C incubator for 24 hours before testing allowing for the stationary phase to be reached. The E. coli stock solution was kept for approximately two weeks in the incubator and was purified every couple of months by streak plating the stock solution and transferring colonies to fresh TSB.

For testing in the log growth phase, one colony (to assure genetic homogeneity) was obtained from a TSA plate after overnight incubation at 37°C and added to 10 mL of sterile TSB in a sterile 15 mL vial. The vial was rapidly vortexed to break up the colony and then the 10 mL solution was added to 90 mL of TSB in a sterile 250 mL glass bottle with a sterile magnetic stir bar. For the *E. coli* DH5α, 100 μL of 1000x concentration carbenicillin antibiotic was added to assure that the *E. coli* DH5α strain was the only bacteria in the stock. The stock solution was incubated at 37°C on a stir-plate to assure constant mixing and oxygen levels throughout the stock.

This solution was used to create the growth curve (section 3.3.2) and kept at 4°C for less than 2 weeks to inoculate future stock solutions.

2 mL of unwashed *E. coli* was used to inoculate 198 mL of phosphate buffer solution (PBS, pH 7.4), for a concentraion of approximately10^6 CFU *E. coli* per mL, for initial testing. Due to the large absorbance values of the unwashed solution, subsequent tests were conducted with 6 mL of washed *E. coli* in 194 mL of PBS. The *E. coli* were washed in PBS by centrifuging 1 mL samples at 5000 rcf for 5 minutes, pouring off the top liquid, adding 1 mL of PBS, vortexing to mix, and centrifuging again. This process was repeated three times.

5.3.3 Determination of Growth Curves

A growth curve was determined for each *E. coli* strain based on the absorbance at 600 nm (OD 600) and cultured colonies. After initial inoculation, the optical density at 600 nm (OD600) was measured every thirty minutes. The OD600 was measured in a 1 mL quartz cuvette and zero was established using sterile TSB (Spectrophotomer HACH, DR 5000). The cuvette was rinsed three times with distilled (DI) water and shaken dry between measurements. Samples were cultured at two points along the curve to compare OD600 values to *E. coli* concentration.

5.3.4 UV Irradiation

E. coli spiked PBS was irradiated with LP and LED sources and the UV-LED prototype was evaluated using *E. coli* K12 as a biodosimeter. All tests were

completed within two hours and irradiated samples were covered to minimize photoreactivation as much as possible.

5.3.4.1 Quasi Collimated Beam Testing

A quasi-collimated beam apparatus was used to expose 40 mL portions of *E. coli* spike PBS at UV fluences ranging from 0 to 20 mJ/cm^2 (Figure 3). Well-mixed sample was poured into a sterile 50 mL glass crystallization dish (2.2 cm diameter) with a sterile magnetic stir bar. The glass dish and stir bar were disinfected under the UV lamp for ten minutes between each test and the same procedure was followed with a sample of sterile water to check for contamination. The sample was placed on a stir plate under the lamps and irradiated for the calculated exposure time using the manual shutter. After irradiation, the sample was poured into a vial and vortexed to mix. Serial dilutions were made, vortexing each dilution for five seconds before making the next dilution. Multiple water samples were tested at each UV fluence in order to assess errors in the measurements.

5.3.4.2 UV-LED Batch System Testing

5-7 mL of *E. coli* spiked PBS was placed in a 10 mL beaker with a sterile magnetic stir bar and exposed to UV doses between 0 and 20 mJ/cm^2 while constantly stirred (Figure 4). The exposure times were determined based on E_{avg} to deliver the desired UV dose.

5.3.4.3 UV-LED Prototype

The UV-LED prototype was evaluated by flowing *E. coli* spiked PBS and *E. coli* spiked natural water (collected from a local pond) through the system. Initial *E. coli* concentration was tested by running the sample through the prototype with the LEDs turned off. Log reduction of *E. coli* was evaluated for multiple flow rates and multiple UV absorbance values. The system was disinfected by flowing 500 mL of 0.6% sodium hypochlorite solution through the tubing and prototype followed by 500 mL of sterile DI water before all rounds of tests.

5.3.5 UV Dose Calculations

In order to provide the appropriate UV fluences, the lamp irradiance and the exposure time necessary was determined prior to the irradiation of samples. Using the sample absorbance, water depth, and measured distance from the UV source to the water surface, the following equations were used to calculate the average sample irradiance (Bolton and Linden, 2003):

$$E'_{avg} = E_o * Petri\ Factor * Reflection\ Factor * Water\ Factor * Divergence\ Factor$$

$$WaterFactor = \frac{1 - 10^{-A*b}}{A * b * In(10)}$$

where E'_{avg} is the average sample irradiance, E_o is the incident irradiance measured with the UV radiometer, A is the sample absorbance and b is the sample depth. Using E'_{avg} and the required UV fluences, the exposure time was calculated:

$$Exposure\ Time\ (s) = \frac{UV\ Fluence\ (mJ/cm^2)}{E'_{avg}\ (mW/cm^2)}$$

The incident irradiance was measured before and after each set of tests with a digital UV radiometer (IL1400A, International Light). The average irradiance was estimated according to Bolton and Linden (Bolton and Linden, 2003). A petri factor of 0.98 and one were used for the LP and LED systems, respectively, and a reflection factor for water of 0.975 was used. The water factor accounted for the UV absorbance of the water through the sample water depth and the UV absorbance of the sample at 254 nm and 266 nm for the LP and LED systems, respectively (measured with a spectrophotometer, HACH DR 5000).

The divergence factor accounted for the divergence of light from the source over the lamp-to-sample distance. The divergence factor was not used for the samples irradiated with the LEDs due to the narrow output (six degrees) of the LEDs used. This assumption was tested by evaluating log inactivation for samples with 1 cm and 2 cm water depths to assure that the divergence factor had no effect on the LED system.

Irradiation time was controlled by a manual shutter for LP tests and by turning on/off the lamps for LED tests. The LP lamps and LEDs were allowed to warm-up for 10 minutes before tests and the LEDs were turned off for a maximum of 10 seconds while tests were being set-up, which did not significantly affect the irradiance. The LP system did not need to be turned off while tests were set up due to the greater distance from the lamps to the sample allowing enough space for a manual shutter to be used.

5.3.6 Determination of *E. coli* Concentration

After irradiation, *E. coli* concentrations were tested using the vacuum filtration method for the first half of testing and spot plating was used for the second half. Comparisons between the two methods showed no significant difference in results and spot plating allowed for testing to be conducted much faster.

5.3.6.1 Vacuum Filtration Method

The vacuum filtraton method was conducted according to standard method #9222 (APHA, 1998). A glass vacuum filtration apparatus was used with a 1000 mL sidearm Erlenmeyer flask. All glassware, pipette tips, agar, and broth were autoclaved for twenty-five minutes and allowed to cool to room temperature before use. A 0.45 μm sterile filter membrane (Whatman #09-529-712) was placed in the vacuum apparatus and 10 mL of sterile 1x phosphate buffer solution (1x PBS, pH 7.4) and 1 mL of sample was added. The PBS was added first to assure even spreading of sample across the filter. The vacuum was turned on until the liquid was removed from the filter apparatus. Using flamed tweezers, the filter membrane was removed from the vacuum apparatus and rolled onto MacConkey agar (Difco #212123) in a 60 x15 mm Petri dish. This process was repeated in duplicate for each dilution (serial dilutions were made with 1x PBS) of each sample rinsing the vacuum filter with 20 mL of sterile DI water between each test. After every ten tests, 10 mL of sterile water was run through the same procedure to check for contamination. The agar plates were then inverted and incubated for 24 hours at 37°C.

5.3.6.2 Spot Plating Method

The spot plating technique allows bacterial colonies to be quantified by dropping a known volume of bacterial suspension onto the surface of a solid agar media (Gaudy et al., 1962). This method is advantageous because four dilutions of five replicates each can be read on one 100 mm diameter plate, which would require twenty 60 mm diameter plates using the vacuum filtration method. There was also less concern for contamination between sample plating.

The spot plating method involved dividing a 100 mm diameter TSA dish into four quadrants by drawing lines with a black sharpie marker on the bottom of the plate. Five 10 μL drops of each sample dilution were then placed in each quadrant using a 2-20 μL pipettor. Once the spots had completely dried, the plates were placed upside down in the 37°C incubator. The plates were incubated for 24 hours before the colonies were counted.

5.4 Data Analysis

For the vacuum filtered samples, the *E. coli* colonies show up metallic red on the MacConkey agar after incubation and these colonies were counted for each 60 mm plate. Colony counts between 20 and 200 were recorded as CFU/mL. Standard Methods states that colonies counts below twenty should be cautiously interpreted and colony counts above 200 are no longer able to be counted due to growth overlap (APHA, 1998). The number of bacterial colonies formed was recorded and log inactivation was calculated as a function of UV dose (spreadsheet in Appendix B).

For the spot plating method, individual spots of a low dilution appeared as one large spot and spots of a high dilution had one, two, or no colonies appear. Spots with 3 to 30 colonies were recorded (CFU/0.01 mL). If two dilutions had results that fell into this range, the lower dilution (more colonies in each spot) was chosen. The colonies were averaged for the five spots and converted to CFU/mL by multiplying by the dilution factor (spreadsheet in Appendix B).

The log reduction (log N_o/N) was calculated for each test based on the initial non-irradiated *E. coli* concentration, N_o, (CFU/mL) and the concentration of *E. coli* post-irradiation, N (CFU/mL). The duplicate tests (for vacuum filtration) and quintuplicate tests (for spot plating) were averaged for a combined log reduction for each sample irradiated. All of the tests conducted for a particular strain of *E. coli* were combined by averaging the log reductions for each similar dose provided.

A paired t-test was performed on the low-pressure and LED *E. coli* K12 inactivation data to evaluate if there is a statistical difference in efficiency between the two UV sources. The paired t-tests were based on a 95% confidence interval on the difference between the means of the LP and LED inactivation at a given dose (2, 5, 10, 15, and 20 mJ/cm^2).

Statistical regressions were performed for three models on the *E. coli* K12 data; logarithmic, second order polynomial, and the Mamane-Linden model (Mamane and Linden, 2005). The Mamane-Linden model takes the shoulder, linear, and tailing sections (frequently found in microbial dose-response curves) into consideration. To model the tailing effect found in the data, the Mamane-Linden model was evaluated:

$$\log\left(\frac{N_d}{N_o}\right) = \frac{1-(1-10^{-k_1 H_o})^{10^d} + a10^{-k_2 H_o}}{1+a}$$

The coefficients were determined from linear trendlines of the data from 0-10 mJ/cm2 (linear portion) and 10-20 mJ/cm2 (tailing portion). The k1 and k2 values are the slopes of the linear and tailing trendlines, respectively. The d value is the y-intercept of the trendline for the linear portion and the a value is 10 taken to the negative power of the y-intercept of the tailing portion. H_o in the model is the dose in mJ/cm^2.

6. Results and Discussion

6.1 Irradiance

6.1.1 Radiometer Measurements

Over the first 10 minutes after start-up, the irradiance of the UV-LEDs decreases by about 7% and the irradiance of the LP lamps increases by about 20%, after which time both sources level out (Figure 4).

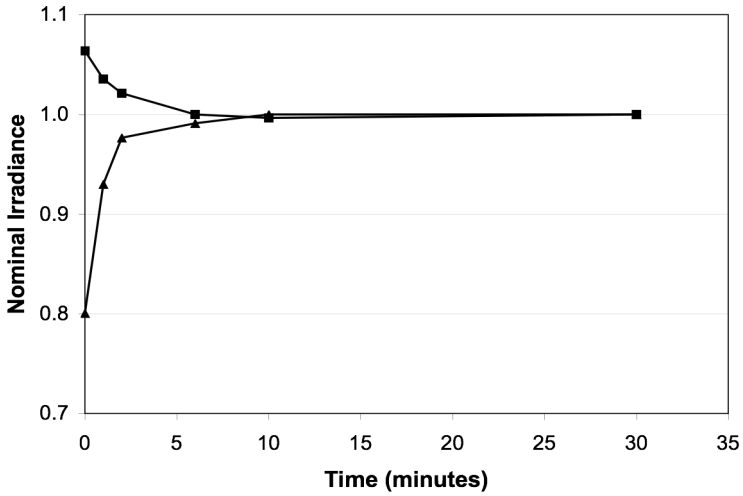

Figure 4. Warm-up time for UV-LEDs (■) versus Low Pressure Lamps (▲)

The irradiance decreases with distance from the UV-LED source; rapidly at small distances and slowly at larger distances from the source to the radiometer detector. Up to five cm, the irradiance can be approximated with the equation in Figure 5.

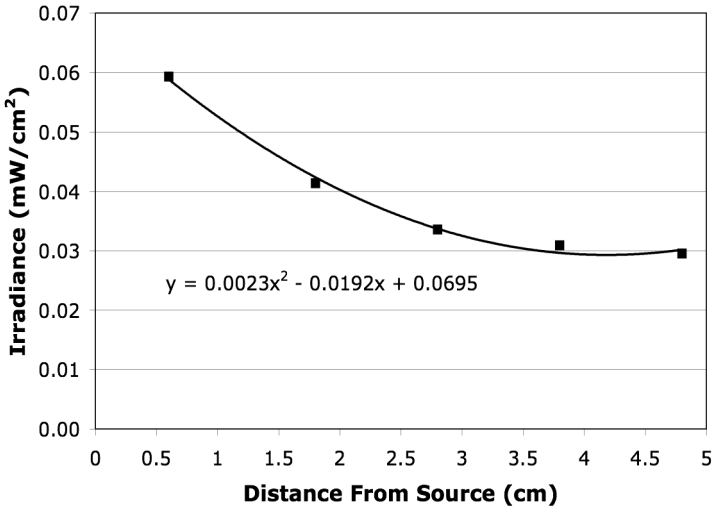

Figure 5. Irradiance over distance for one 265 nm LED

6.1.2 Spectrometer Measurements

Seven lamps from SET were tested with a spectrometer (Ocean Optics USB 2000+). All of the lamps appear to output light at a slightly higher wavelength than rated, particularly the 250 nm lamp (Figure 6). Three of the four 265 nm lamps output light at very similar irradiance at a wavelength of around 266 nm. The fourth 265 nm lamp is about 25 microW/cm2 higher. This could be due to variations in manufacturing or less usage time than the other three lamps. None of the lamps had been run for more than one hour at this point.

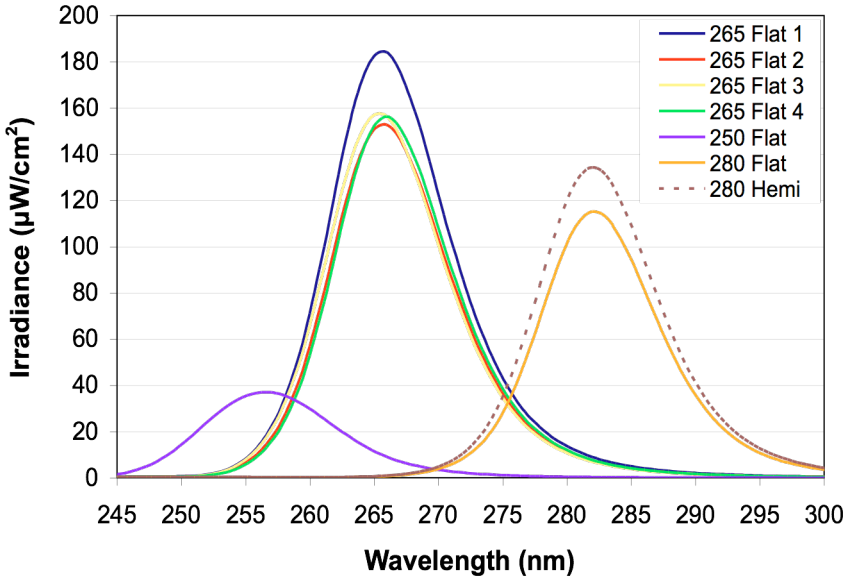

Figure 6. Irradiance of UV-LEDs of various output wavelengths (1mm from source)

The UV-LEDs from SET appear to have a broader bandwidth than the narrow spike at 254 nm produced by low-pressure lamps (Figure 7). The full width at half maximum (FWHM), measured acorss the spectra at 50% of the peak irradiance, is 10.8 nm for the 265 nm LED, which is slightly lower than the manufacturer specification of 12 nm. The broader emission spectra could have implications for system designs, paricularly if very specific wavelengths are desired.

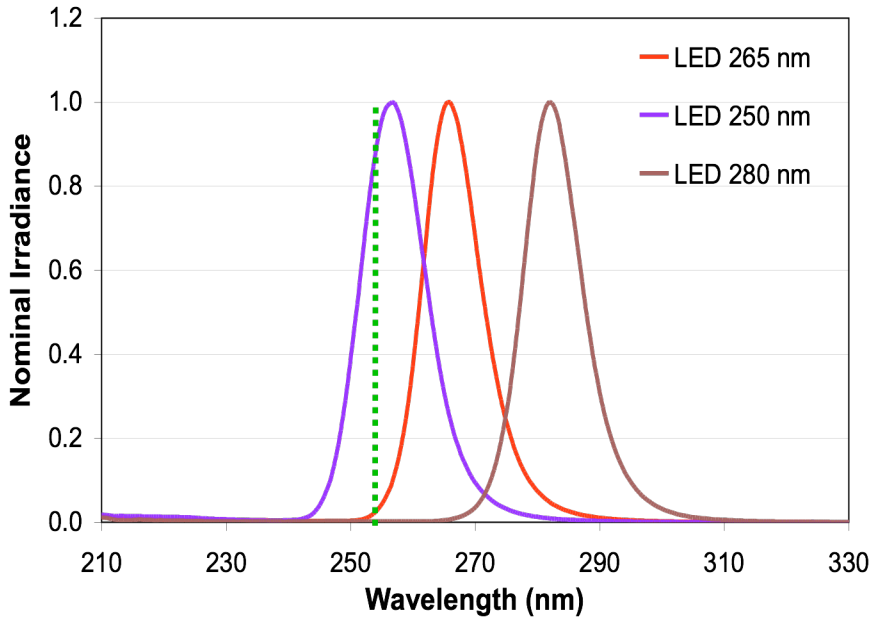

Figure 7. Nominal irradiance of three LEDs compared to the narrow spike of low-pressure lamps

6.2 Actinometry

The actinometry results correlate well with the radiometer data for the low-pressure system and the UV-LED batch system (Figure 8). The difference between the radiometer reading and the average actinometry results were 0.6%, 3.1%, and 16% for the LP and two UV-LED batch system tests, respectively. The radiometer readings were therefore used to determine the dose for all subsequent tests.

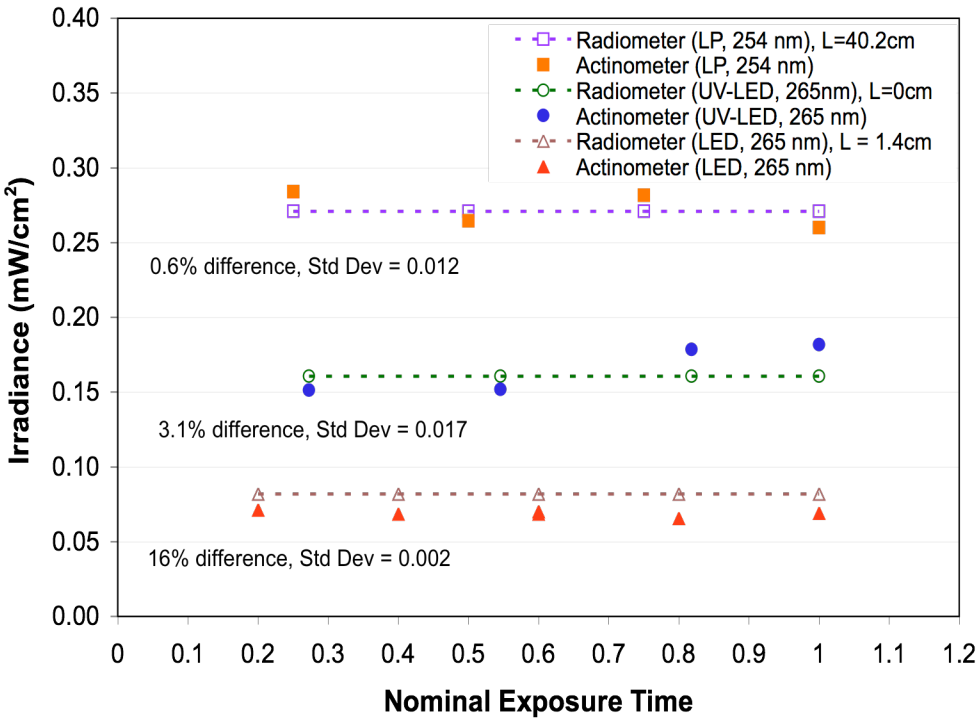

Figure 8. Comparison of Radiometer and Actinometer for LP and LEDs

6.3 Inactivation of E. coli

6.3.1 Microbiological Growth Curves

Based on the data in Figure 9, the OD600 can be used to roughly estimate the *E. coli* concentration (CFU/mL) with the following equations for each strain of *E. coli*:

E. coli lab strain: $(3.2 \times 10^8) \times$ OD600

E. coli DH5α strain: $(1.8 \times 10^8) \times$OD600

E. coli K12 strain: $(5 \times 10^8) \times$OD600

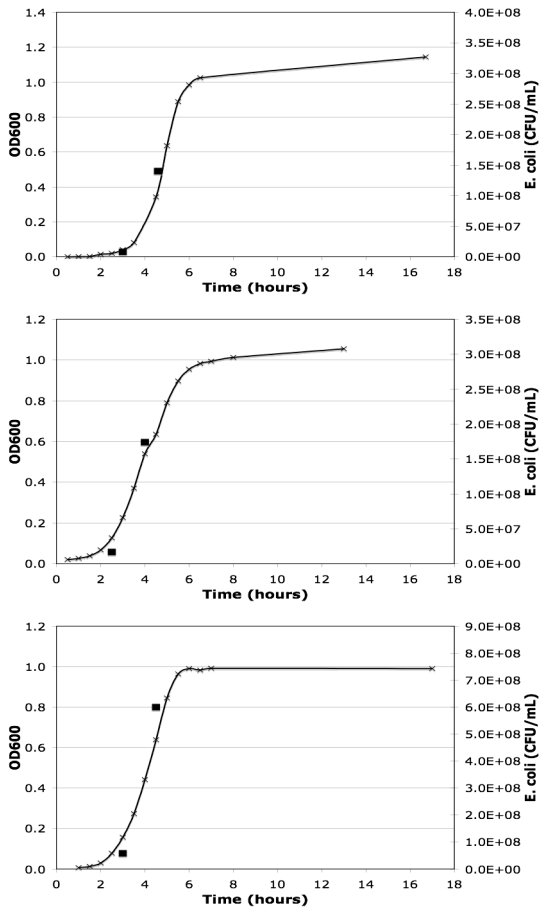

Figure 9. Growth curves for *E. coli* (top to bottom: lab strain, DH5α, K12), OD600 readings (×) and cultured colonies (■)

This information was used to determine the growth phase of the E. coli during tests, which can have a significant effect on the UV sensitivity of the microorganism. As shown by Morton and Haynes, E. coli in the late log phase can be more sensitive to UV by 1-2 log compared to *E. coli* in the early log or stationary phases (Morton and Haynes, 1969).

6.3.2 Low-Pressure versus UV-LEDs

Log reduction of the lab strain appears to be slightly improved for the LED source at low doses and approximately the same at higher doses, based on thirty and eight data points in duplicate for the LED and LP sources respectively (Figure 10). However, testing was stopped after 38 tests due to the lower than expected rate of disinfection for *E. coli*. Actinometry was performed to check the radiometer used to attain the irradiance value used in the dose calculations. The actinometry was within reasonable error, particularly for the low-pressure lamp, and it was determined that radiometer was not a source of error.

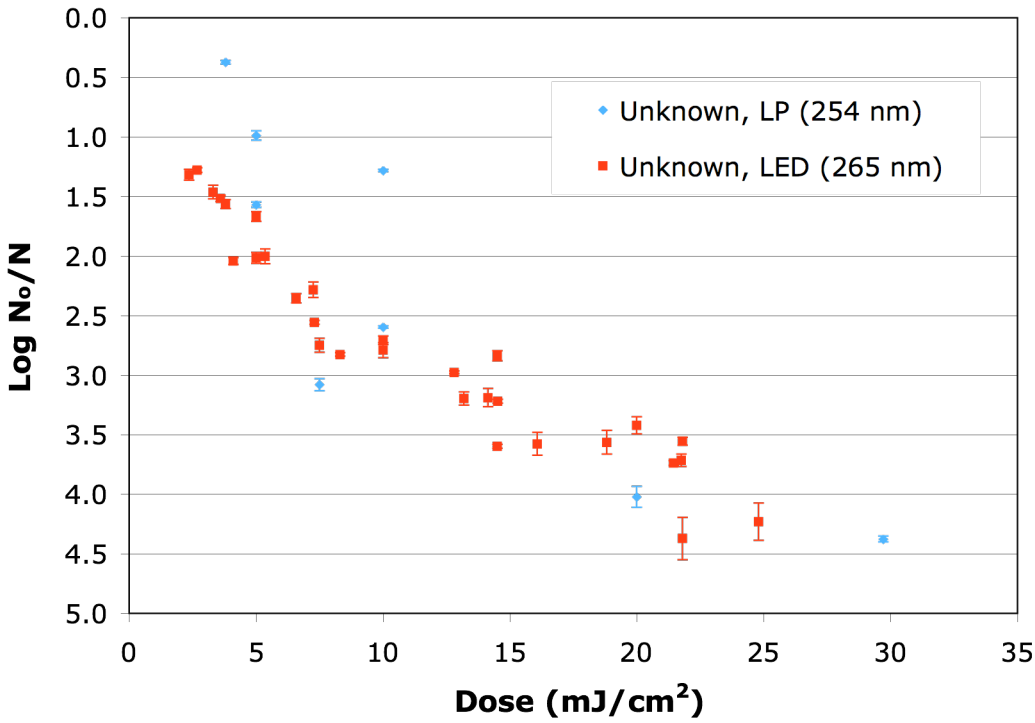

Figure 10. Log reduction of E. coli (lab strain) by irradiation from low-pressure lamps (254 nm) and LEDs (265 nm). Error bars represent one standard deviation of the mean

Sommer et al. (2000) showed that different strains of *E. coli* can have different sensitivities to UV irradiation (Figure 11). To evaluate the method, *E. coli* DH5α, a strain known to be sensitive to UV irradiation, was evaluated in the lab. Few data points were taken due to the rapid kill that was difficult to measure, but the results show that the method used in the lab appears to be within published values for inactivation of *E. coli* (Figure 12).

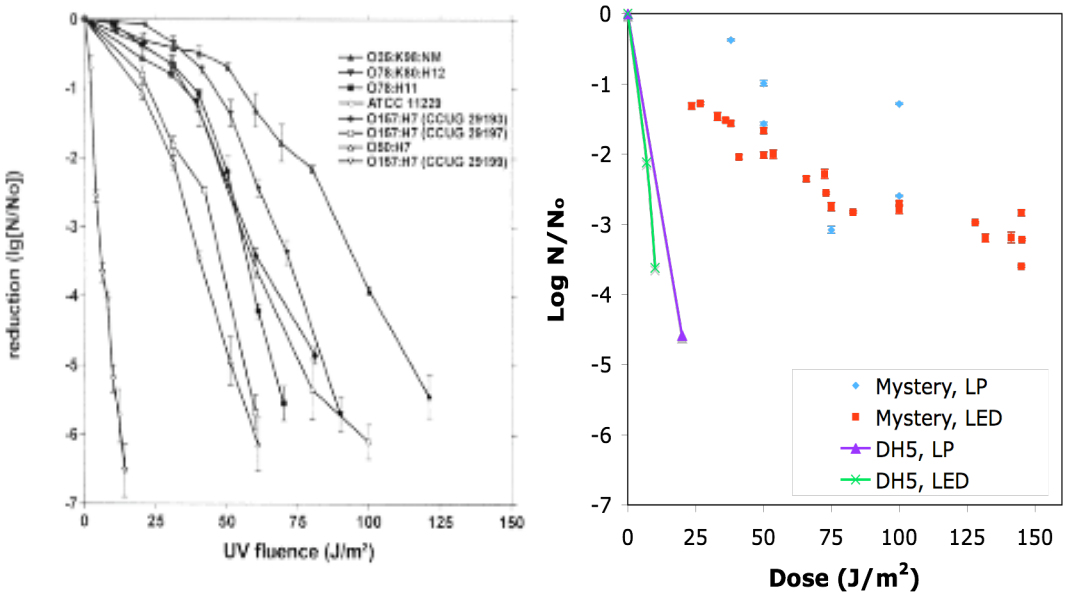

Figure 11. Comparison of inactivation rates of lab *E. coli* strain to DH5α and multiple *E. coli* strains in the literature (Sommer et al., 2000)

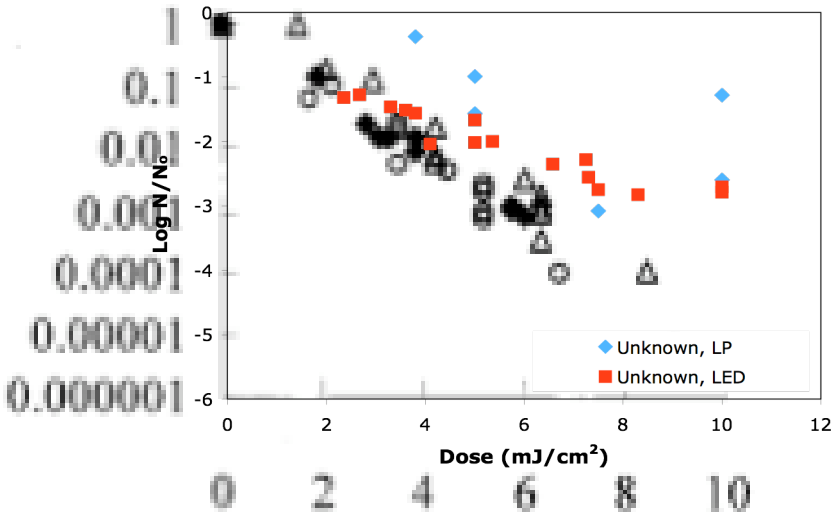

Figure 12. Comparison of inactivation of the lab *E. coli* strain and *E. coli* K12 in the literature (Oguma et al., 2002)

Due to the variance in UV sensitivity based on strain, the results were compared to *E. coli* K12, since that is what the lab strain is thought to be. Inactivation of *E. coli* K12 in the literature, showed that it is less sensitive to UV irradiation than many other strains. However, inactivation of *E. coli* K12 performed by Oguma et al. (2002) does not correspond to the inactivation of the lab *E. coli* strain performed in the lab (Figure 12).

Irradiation tests were performed on *E. coli* at multiple growth phases based on findings by Morton and Haynes (1969) that UV sensitivity varies for microorganisms in different growth phases. The lab *E. coli* strain was evaluated at early log, late log, and stationary phases, but no significant difference was found. This discrepancy could be due to the lab *E. coli* strain not being *E. coli* K12 or the strain could have mutated through years of use in multiple labs. A pure strain of *E. coli* K12 was obtained from ATCC (#29425) and a new round of testing was conducted with the *E. coli* K12 at log growth phase instead of stationary phase based on common

methodology found in the literature. The *E. coli* K12 obtained from ATCC was no more sensitive than the lab *E. coli* strain (Figure 13). The lower sensitivity seen in the results could be due to photoreactivation or data analysis errors, but based on the actinometry, the dose received should be accurate. The difference is small however, and should not affect the goal of this research to compare the efficacy of using LP lamps and UV-LEDs as the irradiation source for disinfecting *E. coli* in water.

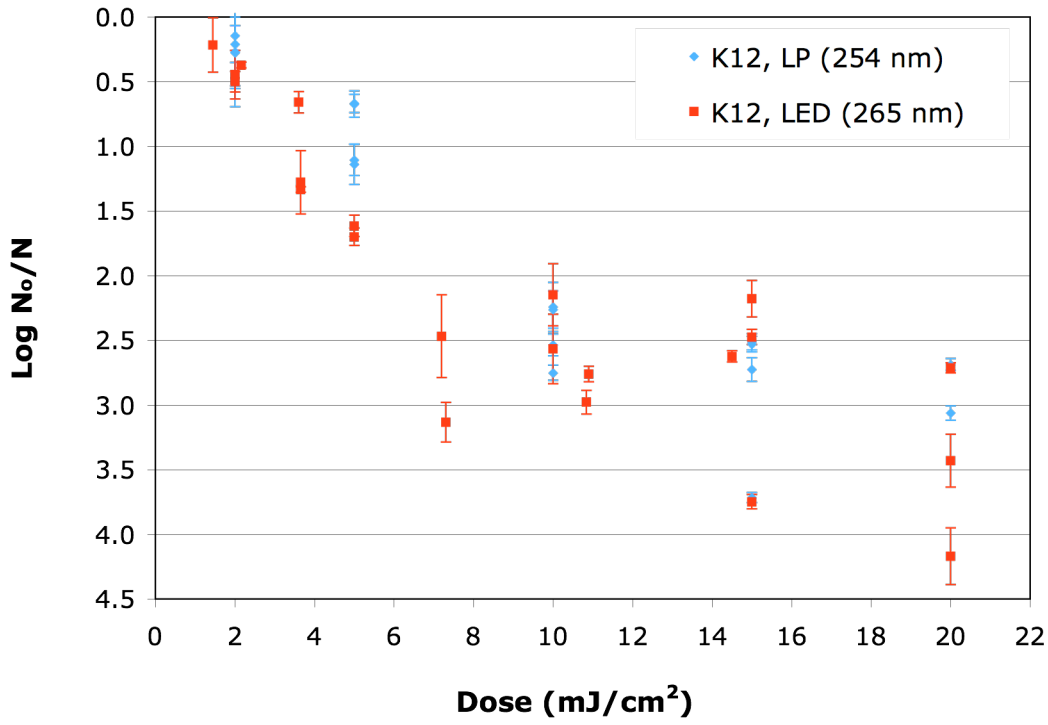

Figure 13. Inactivation of *E. coli* K12 by low-pressure lamps and UV-LEDs. Error bars represent one standard deviation of quintuplicate tests.

The data were modeled using the Mamane-Linden model, and logarithmic and 2nd order polynomial regressions (Mamane and Linden, 2005). The coefficients for the Mamane-Linden model are found in Table 1.

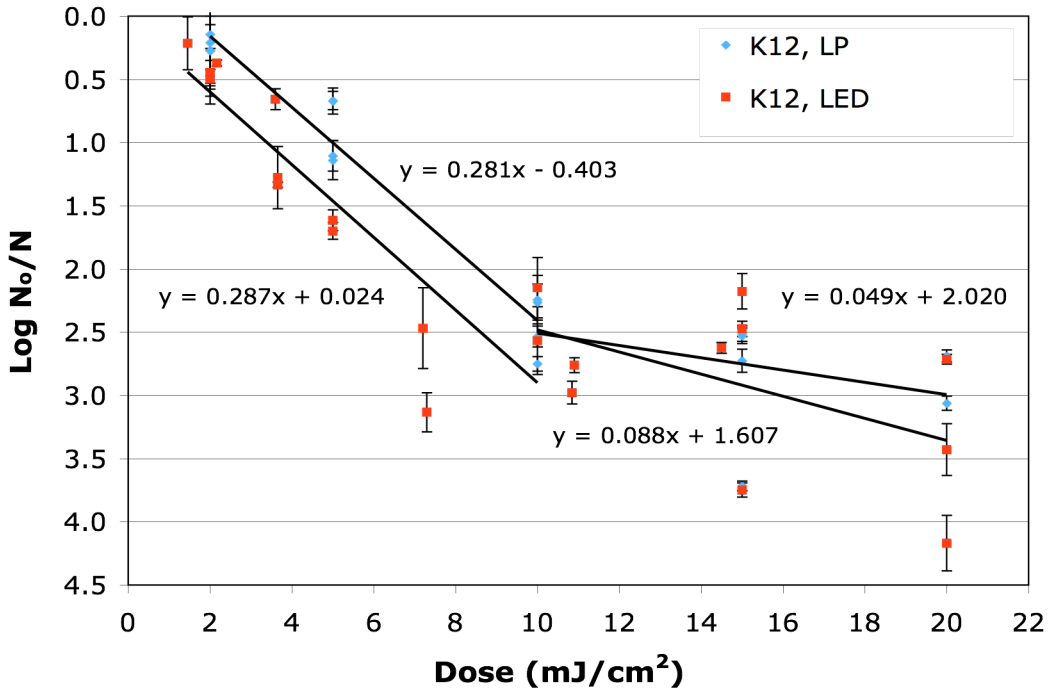

Figure 14. Linear trendlines used to determine coefficients for Mamane-Linden model

Table 1. Coefficients for Mamane-Linden Model

Source	Equation (linear portion)	Equation (tailing portion)	Coefficient	Value
LP	y = 0.281x - 0.403	y = 0.049x + 2.020	k1	0.281
			k2	0.049
			d	0.403
			a	0.0955
LEDs	y = 0.287x + 0.024	y = 0.088x + 1.607	k1	0.287
			k2	0.088
			d	-0.024
			a	0.0247

The resulting Mamane-Linden model can be found in Figure . The three models were evaluated for the *E. coli* K12 inactivation data for the LP and LED sources (Figure 15, Figure 16, Figure 17). R-squared values were calculated and compared for all three models to determine the best model for the data (Table 2). The logarithmic and second order regressions performed slightly better than the Mamane-Linden model for the raw and averaged *E. coli* K12 inactivation data. The logarithmic regression was the best model for the LED data and the second order polynomial regression was the best model for the LP data. The R-squared values were within 4% of each other for the logarithmic and second order models. One model was chosen for both data sets for ease of comparison. The logarithmic model was chosen over the second order polynomial so that dose response predictions greater than twenty mJ/cm^2 can be made.

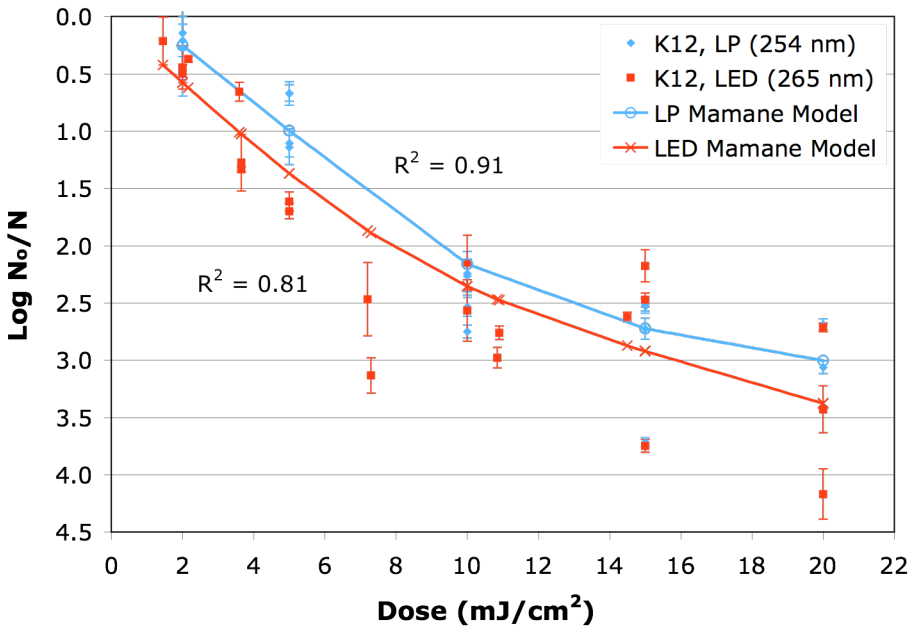

Figure 15. Mamane-Linden model for *E. coli* K12 inactivation data

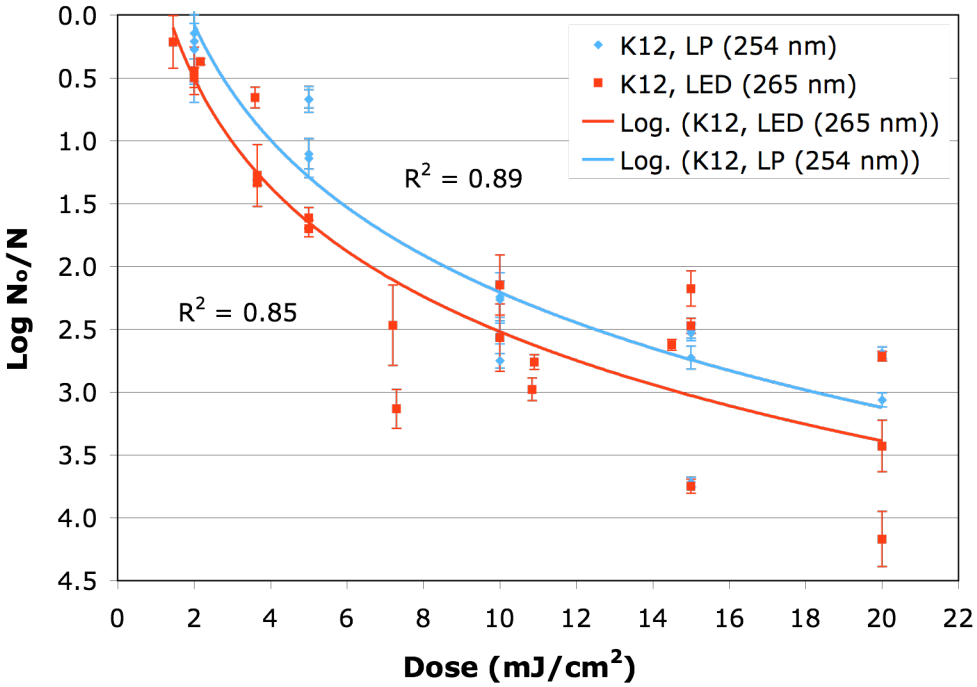

Figure 16. Logarithmic regression for *E. coli* K12 inactivation data

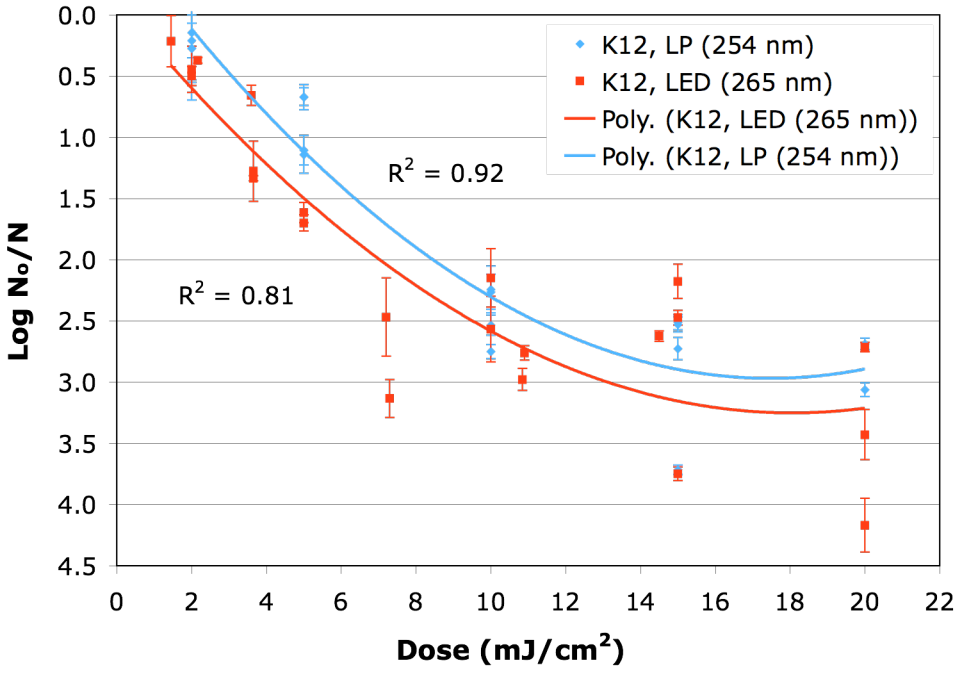

Figure 17. Second order polynomial regression for *E. coli* K12 inactivation data

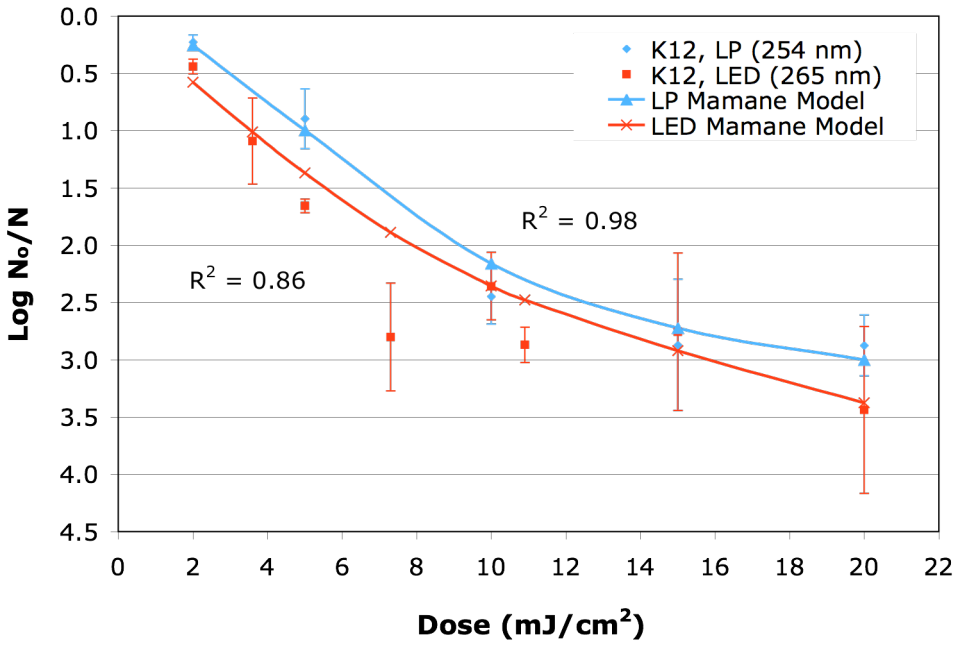

Figure 18. Mamane-Linden model for grouped and averaged *E. coli* K12 data

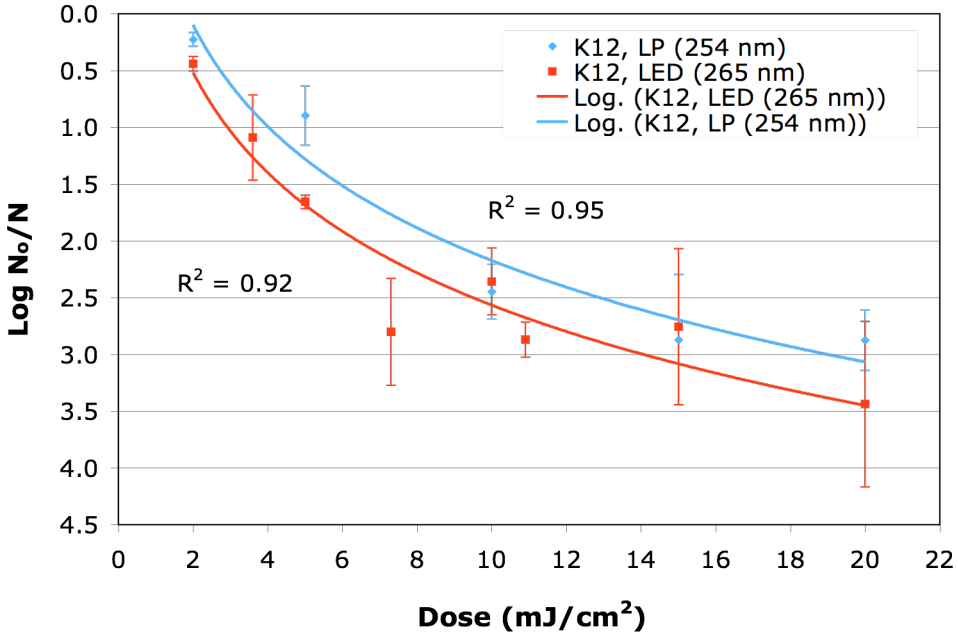

Figure 19. Logarithmic regression for grouped and averaged *E. coli* K12 data

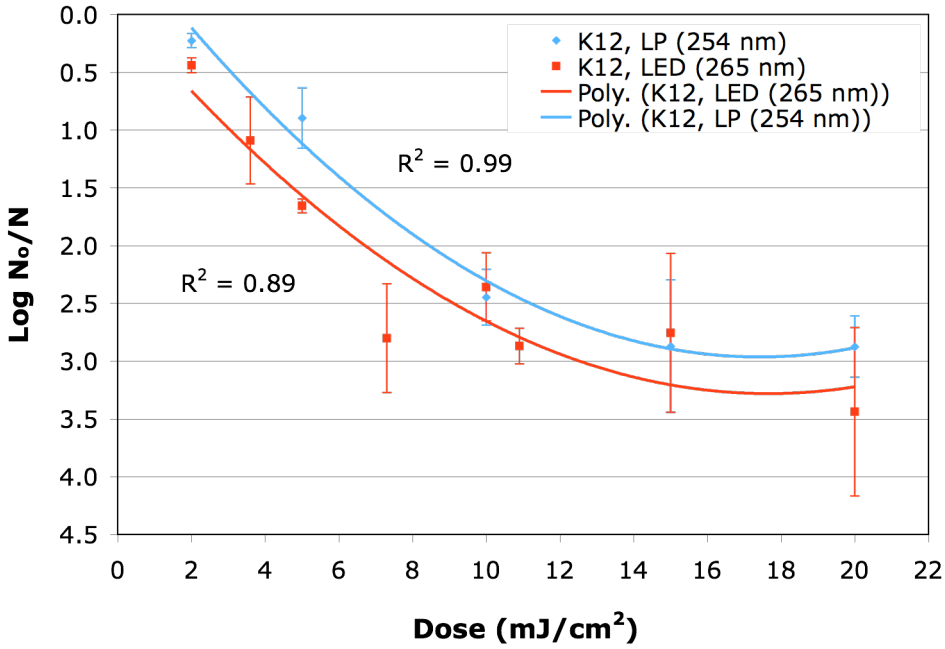

Figure 20. Second order polynomial regression for grouped and averaged *E. coli* K12 inactivation data

Table 2. Comparison of three models for *E. coli* K12 inactivation data

Model	Data Set	Low-Pressure		LEDs	
		P-value	R^2	P-value	R^2
Mamane-Linden	Raw Data	1.19×10^{-9}	0.907	4.21×10^{-9}	0.813
Logarithmic		4.76×10^{-9}	0.889	5.12×10^{-10}	**0.847**
2nd order polynomial		4.18×10^{-9}	**0.924**	6.91×10^{-8}	0.808
Mamane-Linden	Averaged	1.55×10^{-3}	0.976	9.26×10^{-4}	0.859
Logarithmic		4.95×10^{-3}	0.949	1.77×10^{-4}	**0.918**
2nd order polynomial		1.35×10^{-2}	**0.986**	4.05×10^{-3}	0.890

Based on results of paired t-tests, at a 95% confidence, the low-pressure and LED sources are not statistically different for the inactivation of E. coli K12 (Table 3). Tests performed on individual doses, show statistically significant improvement at doses of 2, 5, and 20 mJ/cm^2, but not at doses of 10 and 15 mJ/cm^2 for a 95% confidence.

Table 3. Paired t-test for the *E. coli* K12 inactivation data

	Average Removal		
Dose (mJ/cm^2)	**Low Pressure**	**LED**	**Difference**
2	0.23	0.44	0.21
5	0.90	1.66	0.76
10	2.45	2.36	-0.09
15	2.87	2.80	-0.07
20	2.87	3.44	0.56

Average Difference	0.275
Standard Deviation	0.379
t_o	**1.623**
alpha	0.050
$t_{95\%}$	**2.015**

6.3.3 UV-LED Flow-Through Prototype

The ten-LED prototype was evaluated using biodosimetry with *E. coli* K12. The linear trendlines for log reduction with varying UV absorbance (UVA) values all have a similar slope (within one log reduction per one liter per hour) and the waters

with lower UVA values are disinfected to the same level of waters with higher UVA values at lower flow rates, as expected (Figure 21). The natural water (UVA of 0.259) appears to have a similar response and is in the middle of the PBS samples with UVA values of 0.129 and 0.342).

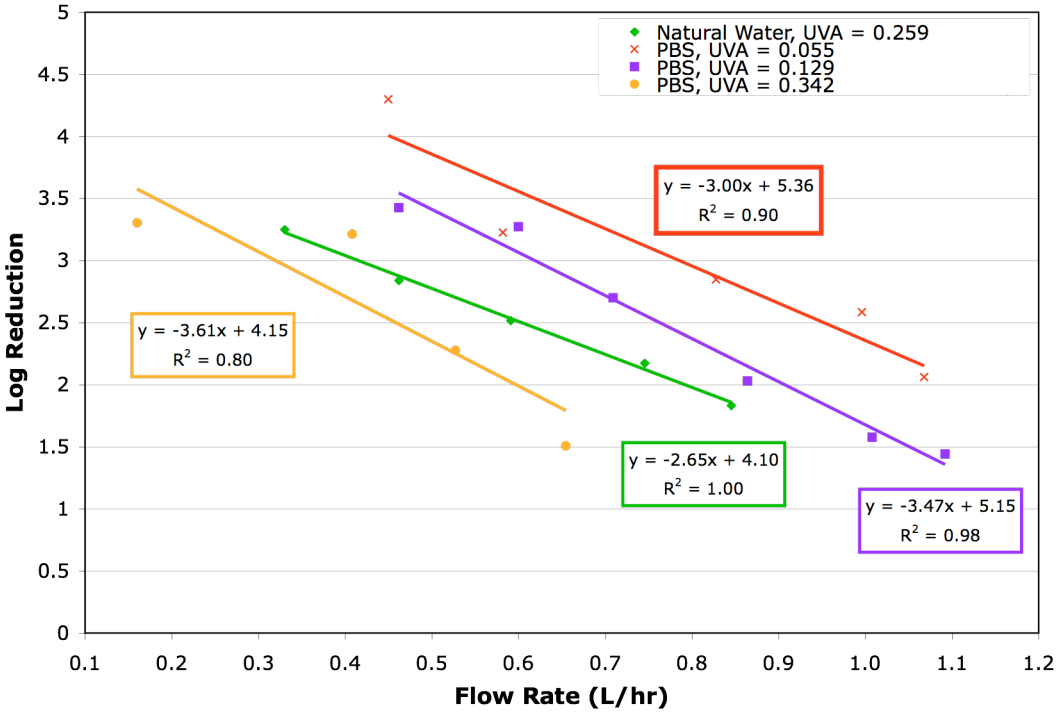

Figure 21. Dose response for multiple flow rates and UVA values of *E. coli* K12 spiked PBS and natural water

In order to compare the prototype to commercial system, the dose provided for a given flow rate in mL/min and influent water UV transmittance (UVT) are needed. The dose was calculated based on the logarithmic regression model (log reduction = 1.25*Ln(Dose) – 0.3665) of the *E. coli* K12 inactivation dose response to UV-LEDs (Figure 22). The UVA values were converted to UVT with the equation $UVT = 10^{-UVA}$. For a UVT of 88%, a dose of ten mJ/cm^2 can be reached with a flow

rate of fourteen mL/min. For a UVT of 74%, the flow rate required for a dose of ten mJ/cm^2 (UVT = 74%) is 11.1 mL/min. This corresponds to a dose of forty mJ/cm^2, the NSF standard for UV disinfection systems, if forty LEDs are used with a flow rate of 11.1 mL/min. Forty LEDs provide 14.4 mW of power, therefore 1.3 mW are needed per mL/min flow rate. This number can be used to size larger systems to compare UV-LEDs to LP systems.

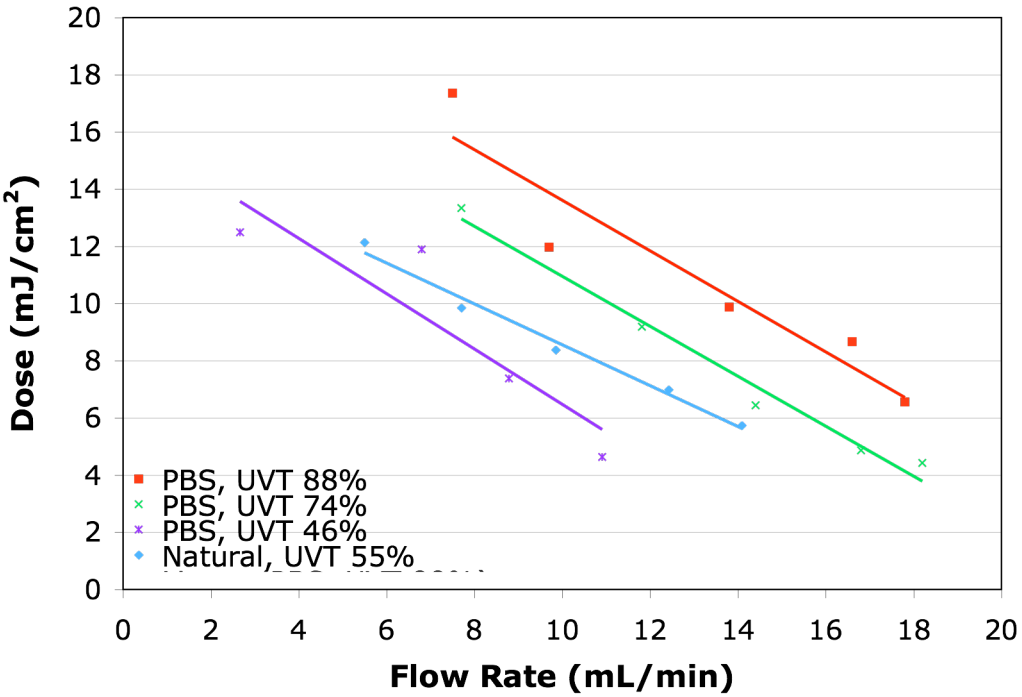

Figure 22. Dose recieved for a given flow rate and UVT for *E. coli* K12 spiked PBS and natural water

6.4 Evaluation of Current and Future UV-LED Technology

LEDs that emit light in the germicidal wavelength range are a relatively new technology and current values for cost, output power, and lifetime do not allow them to be a viable option for the replacement of low-pressure lamps used for drinking water disinfection, especially in developing communities. Based on a household system that needs to provide twenty liters per person per day for a family of four (eighty liters per day total), and a dose of forty mJ/cm^2 and 75% UVT (typical specifications for current LP systems), a comparison was conducted of current UV-LEDs with current LP systems such as the UV-Tube and the Sterilight systems. The base case includes current UV-LED specifications and assumes a constantly running system. The comparison shows the much greater cost of UV-LEDs, both upfront and over time since the lifetime is much lower than the LP systems (Table 4). However, SET and Crystal IS, manufacturers of UV-LEDs, estimate great improvements in the next three to four years. If the projected values manufacturers are aiming for are met, a UV-LED system will be a viable and improved option over current LP systems in three to four years (Table 4). Upfront costs may be higher for larger systems, but since warm-up time is not required for LEDs, the UV-LED systems can be run intermittently, greatly increasing their lifetime and decreasing long-term costs due to fewer lamp replacements (Table 4).

Table 4. Comparison of current and projected future UV-LEDs with LP systems based on cost, lifetime, and power output

	UV-Tube	Sterilight	UV-LEDs			
			Base Case	3-4 year projection		
				Constant	Intermittent	
mW/Lamp (output)	15000	10000	0.36	100	100	100
Lifetime (hrs)	9000	9000	1000	10000	10000	10000
Cost ($/mW)	0.0013	0.0055	664	0.1	0.1	0.1
Flow Rate (mL/min)	6000	1890	55.55	55.55	500	1000
Hours/day			24.0	24.0	2.7	1.3
Total Lifetime (days)			42	417	3750	7500
Total Lifetime (years)			0.11	1.14	10	21
Total mW (output)			72.22	72.22	650	1300
Number of LEDs			201	1	7	13
Upfront lamp cost	20	55	47,943	7	65	130
3 year cost	60	165	1,260,063	21	65	130
20 year cost	389	1,071	8,400,421	123	130	130

Increasing power output will be necessary for systems to utilize a reasonable number of LEDs independent of lamp cost. Each LED requires wiring and other electrical components such as resistors and heat sinking material. More lamps also require a larger system and more materials that will cost more up front. Maintenance will also be more difficult with a larger number of LEDs since each lamp will need to be monitored to detect broken or burned out lamps. This will be particularly important for systems that require a high flow rate, where thousands of LEDs may become difficult to install and maintain. Crystal IS is hoping to have 100 mW (power output) LEDs on the market by 2013. Improving the power output based on manufacturer projections over the next three to four years, shows a large decrease in the number of LEDs required (from over 200 to only one LED for a constantly running household system that would treat eighty liters per day at forty mJ/cm^2 with a UVT as low as 75% (Table 5).

Table 5. Effect of improving output power on the number of LEDs required

Vary Power Output	Base Case	Case 1	Case 2	Case 3	Case 4	Case 5
mW/lamp	0.36	2	5	10	50	100
Number of LEDs	201	37	15	8	2	1

One of the most desired features of LEDs for disinfection systems is their long lifetime, particularly for developing communities, where replacements can be difficult to come across. UV-LEDs in the germicidal wavelength range currently have very low lifetimes of approximately 1,000 hours to 50% power. Manufacturer projections for the next three to four years would offer lifetimes equal to that of LP lamps (10,000 hours by around 2012) (Table 6). However, since they do not need to warm-up, they can be run intermittently, increasing the total lifetime compared to LP systems ten to twenty fold (Table 4).

Table 6. Effect of improving lifetime on the upfront and long-term cost

Vary Lifetime	Base Case	Case 1	Case 2	Case 3	Case 4	Case 5
Lifetime (hrs)	1000	2000	4000	6000	8000	10000
Total lifetime (days)	42	83	167	250	333	417
Total lifetime (years)	0.11	0.23	0.46	0.68	0.91	1.14
3 year cost	1,260,063	630,032	315,016	210,011	157,508	126,006

The most influential improvement to UV-LED disinfection feasibility is cost decrease. Based on manufacturer's three to four year projections, the cost will decrease over 1,000 fold to $0.1 per mW in 2013. The 6,000 percent decrease in three-year cost for a household system, brings the total cost to 190 dollars, which is almost as cheap as the three year cost for the sterilight system lamps at 165 dollars (Table 7, Table 4).

Table 7. Effect of decreasing lamp cost per mW on the upfront and long-term cost

Vary Cost	Base Case	Case 1	Case 2	Case 3	Case 4	Case 5
Cost ($/mW)	664	332	100	10	1	0.1
Upfront lamp cost	47,943	23,975	7,222	722	72	7
3 year cost	1,260,063	630,136	189,800	18,980	1,898	190

Combining projected improvements to power output, lifetime, and cost per mW, result in UV-LEDs being a feasible option and improvement over LP systems around the year 2013 (Table 8). If the projections can be met this will result in a household system that will treat eighty liters per day at 40 mJ/cm^2 (if UVT of water greater than or equal to 75%) for seven dollars of upfront lamp cost, compared to twenty or fifty-five dollars for lamps for the UV-Tube and Sterilight systems, respectively. The cost savings will increase yearly with slightly higher lifetime values of 10,000 hours for the LEDs versus 9,000 hours for the LP lamps. This will result in lower yearly replacement costs.

Table 8. Effect of improving all three parameters; power output, lifetime, and cost

Vary All	Base Case	Case 1	Case 2	Case 3	Case 4	Case 5
mW/lamp	0.36	2	5	10	50	100
Lifetime (hrs)	1000	2000	4000	6000	8000	10000
Cost ($/mW)	664	332	100	10	1	0.1
Total Lifetime (days)	42	83	167	250	333	417
Total Lifetime (years)	0.11	0.23	0.46	0.68	0.91	1.14
Number of LEDs	201	37	15	8	2	1
Total lamp cost (upfront)	47,943	23,975	7,222	722	72	7
Cost for 3 years	1,260,063	315,068	47,450	3,163	237	19

The long-term cost savings can be increased further and the maintenance required to replace burned out lamps can be decreased, by increasing the system flow rate and turning on the lamps intermittently as water is needed (Table 9, Table 4).

Table 9. Effect of increasing flow rate for future UV-LED systems

Vary Flow Rate	Constant	Case F1	Case F2	Case F3	Case F4	Case F5
Flow Rate (mL/min)	55.55	500	1000	1890	5000	6000
Hours/day	24.0	2.7	1.3	0.7	0.3	0.2
Total Lifetime (days)	417	3750	7500	14175	37500	45000
Total Lifetime (years)	1.14	10.27	20.55	38.84	102.74	123.29
Total mW	72.22	650	1300	2457	6500	7800
Number of LEDs	1	7	13	25	65	78
Total lamp cost (upfront)	7	65	130	245.7	650	780

7. Conclusions

UV-LEDs are an effective technology to inactivate *E. coli* in water. A dose of ten mJ/cm^2 produced around two to 2.5-log inactivation for *E. coli* K12. This value is slightly lower than the *E. coli* K12 inactivation data in the literature, but the two sources were able to be compared nonetheless. The UV-LEDs at 265 nm were not found to be statistically different than low-pressure UV sources at all doses. At doses two, five, and twenty there was a statistically significant improvement with 95% confidence. At doses of ten and fifteen, the two sources were not statistically different. Therefore, overall, we can not conclude that UV-LEDs are an improvement over low-pressure sources.

A ten LED prototype served as a proof-of-concept, but currently UV-LEDs in the germicidal wavelength range are much too expensive, low power and have short lifetimes. According to manufacturer projections, however, UV-LEDs should be a viable and economic option within four years.

7.1 Future Research Needs

More research is needed to develop a practical, implementation-ready, water disinfection unit. Specifically, an optimized design specific to family or small community sized systems is needed to make UV-LED disinfection practical. This includes disinfection unit geometry and UV-LED lamp distribution. Testing disinfection effectiveness for other pathogen types is also necessary before UV-LED technology can be utilized for reliable treatment.

The use of UV-LEDs allows for greater design flexibility and multiple reactor geometries should be modeled to optimize a UV-LED system. Currently, UV disinfection systems are modeled using a version of the point-source summation method, including the line source integration (LSI) method (Blatchley, 1997) and the multiple point source summation (MPSS) method (Bolton, 2000).

The point-source summation method simulates a lamp as a series of co-linear point sources of radiation and estimates the intensity of the lamp at any point in the reactor as the sum of the intensity contributions from each point source (Blatchley, 1997):

$$I_\lambda(R,z) = \sum_{i=1}^{n} \frac{\frac{P_\lambda}{n}}{4\pi\rho_i^2} \exp\left[-\left(\sigma_q t_q + \sigma_w\left(R - r_q\right)\right)\frac{\rho_i}{R}\right],$$

where I_λ = radiation intensity at wavelength λ (mW cm^{-2})

R = radial distance from lamp axis to receptor site (cm)

z = vertical distance (cm)

P_λ = lamp output power at wavelength λ (W)

n = number of point sources

ρ_i = distance from *i*th point source to receptor site (cm)

σ_q = absorbance coefficient for quartz sleeve (cm^{-1})

t_q = quartz sleeve thickness (cm)

σ_w = absorbance coefficient for water (cm^{-1})

r_q = quartz sleeve outside radius (cm)

This equation assumes that the lamp radiates in all directions and is submerged under water and protected by a quartz sleeve. For a system that utilizes UV-LEDs, the assumption that the lamps radiate in all directions no longer holds since LEDs are available in various angular outputs such as 6° and 120° for Sensor Electronic Technology's (SET) hemispherical and flat window lens UV-LEDs, respectively. The varying output angles of UV-LEDs requires that $4\pi\rho^2$ term be adjusted and the assumption that all point sources will have effect on all points in the reactor can no longer be made. The reactor can no longer be assumed to be cylindrical either, since that may not be the optimal geometry for a system utilizing UV-LEDs.

LEDs can not be submerged in water due to the configurations of their electrical connections, so the quartz terms (σ_q, t_q, r_q) in equation X, can be replaced by air terms (σ_a, r_a), and because UV light is almost completely transmitted through air, the absorbance coefficient for air can be neglected (Blatchley, 1997).

Testing disinfection effectiveness for other pathogens is also necessary before UV-LED technology can be utilized for reliable treatment. MS2 bacteriophage and adenovirus may be good organisms to evaluate if there is an increase efficiency in inactivation due to different wavelength UV-LEDs. These organisms are also less sensitive to UV disinfection and data for a dose of forty mJ/cm^2 will be possible.

Cited Literature

APHA. *Standard Methods for the Examination of Water and Wastewater, 20th ed.*, American Public Health Association, American Water Works Association, and Water Environment Federation. Washington DC, 1998.

Bettles, T.; Schujman, S.; Smart, J. A.; Liu, W.; Schowalter, L. UV Light Emitting Diodes; Their Applications and Benefits. Proceedings, *International Ultraviolet Association Conference, Los Angeles, CA*. 2007.

Blatchley, E. R., Numerical Modelling of UV Intensity: Application to Collimated-Beam Reactors and Continuous-Flow Systems. Water Research. Vol. 31, No. 9, pp. 2205-2218. 1997.

Bolton, J. R. Calculation of Ultraviolet Fluence Rate Distributions in an Annular Ractor: Significance of Refraction and Reflection. *Wat. Res.* Vol. 34, No. 13, pp. 3315-3324, 2000.

Bolton, J. R., Linden, K. G. Standardization of Methods for Fluence (UV Dose) Determination in Bench-Scale UV Experiments. *Journal of Environmental Engineering.* ASCE. pp. 209-215. 2003.

Chao, Yun-Peng; Chern, Jong-Tzer; Wen, Chin-Sheng; Fu, Hongyong. Construction and Characterization of Therm-Inducible Vectors Derived From Heat-Sensitive lacl Genes in Combination with the T7 A1 Promoter. *Biotechnology and Bioengineering*, Vol. 79, No. 1, 2002.

Cohn, A. R. *The UV Tube as an appropriate water disinfection technology; An assessment of technical performance and protential for dissemination.* Masters Project, University of California, Berkeley, USA. 2002.

Crawford, M. H.; Banas, M. A.; Ross, M. P.; Ruby, D. S.; Nelson, J. S.; Boucher, R.; Allerman, A. A. Final LDRD Report: Ultraviolet Water Purification Systems for Rural Environments and Mobile Applications. *Sandia Report SAND2005-7245.* 2005.

Ducoste, J. J.; Liu, D.; Linden, K. G. Alternative Approaches to Modeling Fluence Distribution and Microbial Inactivation in Ultraviolet Reactors: Lagrangian versus Eulerian. ASCE: *J. Environ. Eng*. 2005.

Fewtrell, L.; Colford, J. M.; Water, Sanitation and Hygiene: Interventions and Diarrhoea. A Systematic Review and Meta –analysis. HNP Discussion Paper. The World Bank. July 2004.

Gaska, R. Deep Ultraviolet Light Emitting Diodes for Water Monitoring and Disinfection. Proceedings, *International Ultraviolet Association Conference, Los Angeles, CA*. 2007.

Hamamoto et al. New water disinfection system using UVA light-emitting diodes. Journal of Applied Microbiology, 103, 2291-2298. 2007.

Linden, K. et al. Enhanced UV Inactivation of Adenoviruses under Polychromatic UV Lamps. *Applied and Environmental Microbiology*, Vol. 73, No. 23, 7571–7574. 2007.

Mamane-Grevetz, H. and Linden, K. G. Relationship between physiochemical properties, aggregation and u.v. inactivation of isolated indigenous spores in water. *Journal of Applied Microbiology.* 98, 351-363, 2005.

Mamane-Gravetz, H.; Linden, K. G.; Cabaj, A.; Sommer, R. Spectral Sensitivity of Bacillus Subtilis Spores and MS2 Coliphage for Validation Testing of UV Reactors for Water Disinfection. *Environ. Sci. Technol*. 30, 7845-7852, 2005.

Morton, R. A., Haynes, R. H. Changes in the Ultraviolet Sensitivity of *Escherichia coli* During Growth in Batch Cultures. *Journal of Bacteriology.* Vol. 97, No. 3, pp. 1379-1385, Mar. 1969.

Pruss, A.; Kay, D.; Fewtrell, L.; Bartram, J. Estimating the burden of disease from water, sanitation, and hygiene at a global level. Environ. Health Perspect. 2002. 110(5), 537-542.

Rahn, R. et al. Quantum Yield of the Iodide-Iodate Chemical Actinometer: Dependence on Wavelength and Concentrations. *Photochem. Photobiol. Sci.,* 2003 Aug; 78 (2): 146-52.

Rahn, R. O., in Reinishch, R. F., ed., *Photochemistry of Macromolecules*, Plenum, New York, 1970, p. 31.

Reygadas, F., Lang, M., Kaser, F., *Point-of-Use Ultraviolet Water Disinfection: An Interdisciplinary Approach to Safe Water for Rural Households of Baja California Sur, Mexico*. Masters Project, University of California, Berkeley, USA. 2006.

SET. UVTOP Technical Data. *Sensor Electronic Technology, Inc.* 2008.

Sinha, R. P.; Häder, D. P. UV-induced DNA damage and repair: a review. *Photochem. Photobiol. Sci.,* 2002, 1, 225-236.

Sobsey, M.D., Stauber, C. E., Casanova, L. M., Brown, J. M., Elliot, M. A., Water Filtration: A Practical, Effective Solution for Providing Sustained Access to Safe Drinking Water in the Developing World. *Environ. Sci. Technol*. Vol. 42, 4261-4267. 2008.

U.S. Environmental Protection Agency (U.S. EPA). 2006. Ultraviolet disinfection

guidance manual. EPA 815-R-06-007, Office of Water, Washington, D.C.

Verhoeven, J. W. Glossary of Terms Used in Photochemistry. *Pure & Appl. Chem.,* Vol. 68, No. 12, pp. 2223-2286, 1996.

WHO. The World Health Report 2002 – Reducing Risks, Promoting Healthy Life. World Health Organization, Geneva, Switzerland. 2002.

Appendix A: Actinometry

Experimental Protocol for UV Dose Measurements with KI Actinometry

Originally Prepared by Jim Bolton and Mihaela Stefan
Bolton Photosciences Inc.

1. KI/KIO_3 Actinometry

The KI/KIO_3 actinometer is very convenient and easy to use for low pressure lamp emissions. The actinometer solution does not absorb above 310 nm and so can be used safely in room light. The overall photochemical reaction is:

$$8\ I^- + IO_3^- + 3\ H_2O + h\nu \longrightarrow 3\ I_3^- + 6\ OH^-$$

The actinometer solution consists of 0.6 M KI and 0.1 M KIO_3 in a 0.01 M $Na_2B_4O_7$ buffer solution. The photoproduct is triiodide ion (I_3^-) which exhibits a strong absorption in UV range and can be accurately quantified at $\lambda = 352$ nm (molar absorption coefficient $\varepsilon = 27{,}636\ M^{-1}\ cm^{-1}$ in a 0.6 M KI/0.1 M KIO_3 solution), where the actinometer's components do not interfere. The quantum yield of this actinometer is 0.60 at 254 nm.

For example, for 5.0 mL actinometer solution in a 10 mL beaker (cross-sectional area 3.80 cm^2), the absorbance at 352 nm (in a 1 cm × 1 cm quartz cuvette) before irradiation is found to be 0.021 – call this A_{352}(blank). After irradiation for 3.0 min, the absorbance at 352 nm is 0.526 – call this A_{352}(sample). The following calculations illustrate how the photon irradiance and the irradiance are calculated:

$[I_3^-] = [A_{352}(\text{sample}) - A_{352}(\text{blank})]/27{,}636 = (0.526 - 0.021)/27{,}636$
$= 1.827 \times 10^{-5}$ M

moles $I_3^- = [I_3^-] \times V(\text{L}) = 1.827 \times 10^{-5} \times 0.005 = 9.137 \times 10^{-8}$ moles

einsteins (moles of photons) = moles $I_3^- / \Phi = 9.137 \times 10^{-8} / 0.60$
$= 1.523 \times 10^{-7}$ einsteins

photon irradiance (E_p') = einsteins/(area × time)
$= 1{,}523 \times 10^{-7} / (3.80\ cm^2 \times 180\ s) = 2{,}226 \times 10^{-10}$ einstein $s^{-1}\ cm^{-2}$

irradiance (E') = E_p' × photon energy at 253.7 nm ($U_{253.7}$)

The irradiance must be corrected for the 2.5% that is reflected from the water surface, so the incident irradiance on the water surface is:

E'(corrected) = E'(uncorrected)/0.975
$= (2.226 \times 10^{-10} \times 471{,}576)/0.975$ J $einstein^{-1}$
$= 1.077 \times 10^{-4}$ W $cm^{-2} = 0.1077$ mW cm^{-2}

A general formula for the irradiance is:

$$E' = 29.17 \frac{[A_{352}(\text{sample}) - A_{352}(\text{blank})] \times V(\text{mL})}{Area(\text{cm}^2) \times Exposure\ time(\text{s})}\ (\text{mW cm}^{-2})$$

where the symbols are defined above.

The following procedure should be used for the actinometry test.

a. 100 mL of the KI/KIO_3 actinometry stock solution is prepared by weighing out 9.96 g of KI, 2.14 g of KIO_3 and 0.381 g of sodium tetraborate ($Na_2B_4O_7 \cdot 10H_2O$) (This generates a solution that is 0.60 M in KI, 0.10 M in KIO_3 and 0.01 M in $Na_2B_4O_7 \cdot 10H_2O$). Dissolve in about 60 mL of distilled water and add to a 100 mL volumetric flask and make up to 100 mL with distilled water. The solution should be made up fresh each time and should not be used after standing for more than 4 h.
b. Using a caliper (if possible) measure the internal diameter of a 10 mL beaker and hence calculate the cross-sectional area (*Area*).
c. Measure the absorbance of the actinometry stock solution in a 10 mm pathlength quartz cell at 300 nm and 352 nm. These values should be approximately 0.58 and 0.02, respectively. Call the latter value A_{352}(blank).
d. Measure the irradiance at the center of the beam with the radiometer. The irradiance should be approximately 0.1 – 0.3 mW/cm^2 – call this *E*(before).
e. Add 5.0 mL of the actinometry stock solution and the 3 mm × 12 mm Teflon-coated stir bar to a 10 mL beaker, place the beaker in the center of the beam at the same position as the radiometer detector head, and raise the platform so that the top of the solution to be irradiated will be at the same level as the reference marker on the radiometer detector head.
f. Irradiate for an *exposure time* of 2.5 min (this is for an irradiance of 0.1 mW/cm^2; adjust this time according your irradiance level) and measure the absorbance at 352 nm – call this A_{352}(sample).
g. Repeat (f) for exposure times of 2 and 3 times the time exposed in f (e.g. 5.0 min and 7.5 min for the example given).
h. Replace the beaker with the radiometer detector; lower the platform to the same level as in (d) and record the meter reading – call this *E*(after).
i. Calculate the irradiance using the above formula.

Appendix B: *E. coli* Inactivation Data

K12, log phase, LED	Test 1				Test 2				Test 3				
L (cm)	1.4	source to water surface			1.4				1.4				
1 (cm)	1.9	water depth			1.9				1.9				
a (1/cm)	0.368	UVA at 266			0.08				0.07				
Petri Factor	1				1				1				
Reflection Factor	0.975	for water			0.975				0.975				
Water Factor	0.497				0.844				0.861				
Divergence Factor	NA				NA				NA				
E_o (mW/cm2) at 254nm	0.102	incidence irradiance			0.105				0.1				
E_o (mW/cm²) at 266nm	0.0844				0.0868				0.0827				
E'_{avg} (mW/cm2)	0.0409	average irradiance			0.0714				0.0695				
UV Dose (ml/cm²)	0	1.45	2.16	3.65	0	3.65	7.3	10.84	0	3.6	7.2	10.9	14.5
Exposure time (h:m:s)		0:00:35	0:00:53	0:01:29	0:00:00	0:00:51	0:01:42	0:02:32	0:00:00	0:00:52	0:01:44	0:02:37	0:03:29
Colonies (per plate)													
A	7	4	22	27	11	4	7	10	7	14	4	19	20
B	4	2	22	25	13	6	5	10	8	19	5	13	20
C	5	4	25	24	13	10	9	15	8	22	4	15	25
D	4	2	23	25	13	3	11	15	9	21	11	15	20
E	7	6	23	24	7	11	12	11	12	22	1	15	20
Dilution factor	6	6	5	4	6	5	3	3	6	5	4	3	3
Volume plated (mL)	0.01	0.01	0.01	0.01	0.01	0.01	0.01	0.01	0.01	0.01	0.01	0.01	0.01
Colonies per mL													
A	7.0E+08	4.0E+08	2.2E+08	2.7E+07	1.1E+09	4.0E+07	7.0E+05	1.0E+06	7.0E+08	1.4E+08	4.0E+06	1.9E+06	2.0E+06
B	4.0E+08	2.0E+08	2.2E+08	2.5E+07	1.3E+09	6.0E+07	5.0E+05	1.0E+06	8.0E+08	1.9E+08	5.0E+06	1.3E+06	2.0E+06
C	5.0E+08	4.0E+08	2.5E+08	2.4E+07	1.3E+09	1.0E+08	9.0E+05	1.5E+06	8.0E+08	2.2E+08	4.0E+06	1.5E+06	2.5E+06
D	4.0E+08	2.0E+08	2.3E+08	2.5E+07	1.3E+09	3.0E+07	1.1E+06	1.5E+06	9.0E+08	2.1E+08	1.1E+07	1.5E+06	2.0E+06
E	7.0E+08	6.0E+08	2.3E+08	2.4E+07	7.0E+08	1.1E+08	1.2E+06	1.1E+06	1.2E+09	2.2E+08	1.0E+06	1.5E+06	2.0E+06
Average (CFU/mL)	5.4E+08	3.6E+08	2.3E+08	2.5E+07	1.1E+09	6.8E+07	8.8E+05	1.2E+06	8.8E+08	2.0E+08	5.0E+06	1.5E+06	2.1E+06
Log Reduction													
A	-0.1127	0.1303	0.3900	1.3010	0.0155	1.4548	3.2118	3.0569	0.0994	0.7984	2.3424	2.6657	2.6435
B	0.1303	0.4314	0.3900	1.3345	-0.0570	1.2788	3.3579	3.0569	0.0414	0.6657	2.2455	2.8305	2.6435
C	0.0334	0.1303	0.3345	1.3522	-0.0570	1.0569	3.1027	2.8808	0.0414	0.6021	2.3424	2.7684	2.5465
D	0.1303	0.4314	0.3707	1.3345	-0.0570	1.5798	3.0155	2.8808	-0.0098	0.6223	1.9031	2.7684	2.6435
E	-0.1127	-0.0458	0.3707	1.3522	0.2118	1.0155	2.9777	3.0155	-0.1347	0.6021	2.9445	2.7684	2.6435
Average	0.0137	0.2155	0.3711	1.3349	0.0112	1.2772	3.1331	2.9782	0.0075	0.6581	2.3556	2.7603	2.6241
Error (+)	0.1166	0.2158	0.0188	0.0173	0.2006	0.3026	0.2248	0.0787	0.0918	0.1403	0.5889	0.0703	0.0194
Error (-)	0.1264	0.2613	0.0367	0.0338	0.0683	0.2616	0.1554	0.0974	0.1422	0.0560	0.4525	0.0946	0.0775

K12, log phase, LED	Test 1				Test 2				Test 3				
L (cm)	1.4	source to water surface			1.4				1.4				
l (cm)	1.9	water depth			1.9				1.9				
a (1/cm)	0.368	UVA at 266			0.08				0.07				
Petri Factor	1				1				1				
Reflection Factor	0.975	for water			0.975				0.975				
Water Factor	0.497				0.844				0.861				
Divergence Factor	NA				NA				NA				
E_o (mW/cm2) at 254nm	0.102	incidence irradiance			0.105				0.1				
E_o (mW/cm^2) at 266nm	0.0844				0.0868				0.0827				
E'_{avg} (mW/cm2)	0.0409	average irradiance			0.0714				0.0695				
UV Dose (mJ/cm^2)	0	1.45	2.16	3.65	0	3.65	7.3	10.84	0	3.6	7.2	10.9	14.5
Exposure time (h:m:s)		0:00:35	0:00:53	0:01:29	0:00:00	0:00:51	0:01:42	0:02:32	0:00:00	0:00:52	0:01:44	0:02:37	0:03:29
Colonies (per plate)													
A	7	4	22	27	11	4	7	10	7	14	4	19	20
B	4	2	22	25	13	6	5	10	8	19	5	13	20
C	5	4	25	24	13	10	9	15	8	22	4	15	25
D	4	2	23	25	13	3	11	15	9	21	11	15	20
E	7	6	23	24	7	11	12	11	12	22	1	15	20
Dilution factor	6	6	5	4	6	5	3	3	6	5	4	3	3
Volume plated (mL)	0.01	0.01	0.01	0.01	0.01	0.01	0.01	0.01	0.01	0.01	0.01	0.01	0.01
Colonies per mL													
A	7.0E+08	4.0E+08	2.2E+08	2.7E+07	1.1E+09	4.0E+07	7.0E+05	1.0E+06	7.0E+08	1.4E+08	4.0E+06	1.9E+06	2.0E+06
B	4.0E+08	2.0E+08	2.2E+08	2.5E+07	1.3E+09	6.0E+07	5.0E+05	1.0E+06	8.0E+08	1.9E+08	5.0E+06	1.3E+06	2.0E+06
C	5.0E+08	4.0E+08	2.5E+08	2.4E+07	1.3E+09	1.0E+08	9.0E+05	1.5E+06	8.0E+08	2.2E+08	4.0E+06	1.5E+06	2.5E+06
D	4.0E+08	2.0E+08	2.3E+08	2.5E+07	1.3E+09	3.0E+07	1.1E+06	1.5E+06	9.0E+08	2.1E+08	1.1E+07	1.5E+06	2.0E+06
E	7.0E+08	6.0E+08	2.3E+08	2.4E+07	7.0E+08	1.1E+08	1.2E+06	1.1E+06	1.2E+09	2.2E+08	1.0E+06	1.5E+06	2.0E+06
Average (CFU/mL)	5.4E+08	3.6E+08	2.3E+08	2.5E+07	1.1E+09	6.8E+07	8.8E+05	1.2E+06	8.8E+08	2.0E+08	5.0E+06	1.5E+06	2.1E+06
Log Reduction													
A	-0.1127	0.1303	0.3900	1.3010	0.0155	1.4548	3.2118	3.0569	0.0994	0.7984	2.3424	2.6657	2.6435
B	0.1303	0.4314	0.3900	1.3345	-0.0570	1.2788	3.3579	3.0569	0.0414	0.6657	2.2455	2.8305	2.6435
C	0.0334	0.1303	0.3345	1.3522	-0.0570	1.0569	3.1027	2.8808	0.0414	0.6021	2.3424	2.7684	2.5465
D	0.1303	0.4314	0.3707	1.3345	-0.0570	1.5798	3.0155	2.8808	-0.0098	0.6223	1.9031	2.7684	2.6435
E	-0.1127	-0.0458	0.3707	1.3522	0.2118	1.0155	2.9777	3.0155	-0.1347	0.6021	2.9445	2.7684	2.6435
Average	0.0137	0.2155	0.3711	1.3349	0.0112	1.2772	3.1331	2.9782	0.0075	0.6581	2.3556	2.7603	2.6241
Error (+)	0.1166	0.2158	0.0188	0.0173	0.2006	0.3026	0.2248	0.0787	0.0918	0.1403	0.5889	0.0703	0.0194
Error (-)	0.1264	0.2613	0.0367	0.0338	0.0683	0.2616	0.1554	0.0974	0.1422	0.0560	0.4525	0.0946	0.0775

K12, log phase, LED	Test 4					Test 5										
L (cm)	1.4					1.4										
l (cm)	1.9					1.9										
a (1/cm)	0.082					0.042										
Petri Factor	1					1										
Reflection Factor	0.975					0.975										
Water Factor	0.840					0.914										
Divergence Factor	NA					NA										
E_o (mW/cm2) at 254nm	0.09					0.091										
E_o (mW/cm²) at 266nm	0.0744					0.0753										
E'_{AVG} (mW/cm2)	0.0610					0.0670										
UV Dose (mJ/cm²)	0	15	20	25		0	2	15	2	15	10	5	20	10		Beaker moved?
Exposure time (h:m:s)	0:00:00	0:04:06	0:05:28	0:06:50			0:00:30	0:03:44	0:00:30	0:03:44	0:02:29	0:01:15	0:01:15	0:04:58	0:02:29	0:04:58
Colonies (per plate)																
A	12	24	9	6		12	31	7	5	35	7	29	20	2	4	20
B	10	18	10	6		14	28	5	4	33	13	25	20	3	3	19
C	12	20	4	5		8	45	10	3	31	9	19	17	4	3	22
D	13	20	6	4		9	31	5	2	33	3	24	22	6	5	18
E	12	24	15	4		9	32	9	6	44	9	31	26	6	1	22
Dilution factor	6	2	2	2		6	5	4	6	3	4	4	4	3	4	3
Volume plated (mL)	0.01	0.01	0.01	0.01		0.01	0.01	0.01	0.01	0.01	0.01	0.01	0.01	0.01	0.01	0.01
Colonies per mL																
A	1.2E+09	2.4E+05	9.0E+04	6.0E+04		1.2E+09	3.1E+08	7.0E+06	5.0E+08	3.5E+06	7.0E+06	2.9E+07	2.0E+07	2.0E+05	4.0E+06	2.0E+06
B	1.0E+09	1.8E+05	1.0E+05	6.0E+04		1.4E+09	2.8E+08	5.0E+06	4.0E+08	3.3E+06	1.3E+07	2.5E+07	2.0E+07	3.0E+05	3.0E+06	1.9E+06
C	1.2E+09	2.0E+05	4.0E+04	5.0E+04		8.0E+08	4.5E+08	1.0E+07	3.0E+08	3.1E+06	9.0E+06	1.9E+07	1.7E+07	4.0E+05	3.0E+06	2.2E+06
D	1.3E+09	2.0E+05	6.0E+04	4.0E+04		9.0E+08	3.1E+08	5.0E+06	2.0E+08	3.3E+06	3.0E+06	2.4E+07	2.2E+07	6.0E+05	5.0E+06	1.8E+06
E	1.2E+09	2.4E+05	1.5E+05	4.0E+04		9.0E+08	3.2E+08	9.0E+06	6.0E+08	4.4E+06	9.0E+06	3.1E+07	2.6E+07	6.0E+05	1.0E+06	2.2E+06
Average (CFU/mL)	1.2E+09	2.1E+05	8.8E+04	5.0E+04		1.0E+09	3.3E+08	7.2E+06	4.0E+08	3.5E+06	8.2E+06	2.6E+07	2.1E+07	4.2E+05	3.2E+06	2.0E+06
Log Reduction																
A	-0.0073	3.6917	4.1176	4.2937		-0.0621	0.5257	2.1719	0.3181	2.4730	2.1719	1.5546	1.7160	3.7160	2.4150	2.7160
B	0.0719	3.8166	4.0719	4.2937		-0.1291	0.5699	2.3181	0.4150	2.4985	1.9031	1.6191	1.7160	3.5399	2.5399	2.7383
C	-0.0073	3.7709	4.4698	4.3729		0.1139	0.3638	2.0170	0.5399	2.5257	2.0628	1.7383	1.7866	3.4150	2.5399	2.6746
D	-0.0421	3.7709	4.2937	4.4698		0.0628	0.5257	2.3181	0.7160	2.4985	2.5399	1.6368	1.6746	3.2389	2.3181	2.7618
E	-0.0073	3.6917	3.8958	4.4698		0.0628	0.5119	2.0628	0.2389	2.3736	2.0628	1.5257	1.6021	3.2389	3.0170	2.6746
Average	0.0016	3.7483	4.1698	4.3800		0.0097	0.4994	2.1776	0.4456	2.4739	2.1481	1.6149	1.6991	3.4297	2.5660	2.7131
Error (+)	0.0703	0.0683	0.3000	0.0898		0.1043	0.0705	0.1405	0.2704	0.0518	0.3918	0.1234	0.0875	0.2863	0.4511	0.0487
Error (-)	0.0436	0.0567	0.2740	0.0863		0.1388	0.1356	0.1605	0.2067	0.1003	0.2450	0.0892	0.0970	0.1908	0.2479	0.0384

K12, log phase, LP	Test 1		Test 2			Test 3			Test 4	
L (cm)	40.8		40.8			40.8			40.8	
l (cm)	2.52		2.52			2.52			2.52	
a (1/cm)	0.375		0.088			0.065			0.098	
Petri Factor	0.98		0.98			0.98			0.98	
Reflection Factor	0.975		0.975			0.975			0.975	
Water Factor	0.4074		0.7831			0.8331			0.7627	
Divergence Factor	0.9418		0.9418			0.9418			0.9418	
E_o (mW/cm2) at 254nm	0.272		0.28			0.27			0.26	
E'_{avg} (mW/cm2)	0.0997		0.1973			0.2024			0.1784	
UV Dose (mJ/cm^2)	0	2	0	5	10	15	0	5	10	15	20	0	2
Exposure time (h:m:s)	0:00:20		0:00:00	0:00:25	0:00:51	0:01:16	0:00:00	0:00:25	0:00:49	0:01:14	0:01:39	0:00:00	0:00:11
Colonies (per plate)													
A	9	1	12	6	28	26	7	9	33	30	8	10	9
B	4	4	17	11	20	24	8	6	31	24	8	17	5
C	5	9	8	15	26	28	9	9	24	33	7	12	7
D	8	6	20	13	26	29	9	5	30	29	8	11	7
E	5	8	14	9	27	30	14	9	21	24	10	12	12
Dilution factor	6	6	6	5	3	2	6	5	3	3	3	6	6
Volume plated (mL)	0.01	0.01	0.01	0.01	0.01	0.01	0.01	0.01	0.01	0.01	0.01	0.01	0.01
Colonies per mL													
A	9.0E+08	1.0E+08	1.2E+09	6.0E+07	2.8E+06	2.6E+05	7.0E+08	9.0E+07	3.3E+06	3.0E+06	8.0E+05	1.0E+09	9.0E+08
B	4.0E+08	4.0E+08	1.7E+09	1.1E+08	2.0E+06	2.4E+05	8.0E+08	6.0E+07	3.1E+06	2.4E+06	8.0E+05	1.7E+09	5.0E+08
C	5.0E+08	9.0E+08	8.0E+08	1.5E+08	2.6E+06	2.8E+05	9.0E+08	9.0E+07	2.4E+06	3.3E+06	7.0E+05	1.2E+09	7.0E+08
D	8.0E+08	6.0E+08	2.0E+09	1.3E+08	2.6E+06	2.9E+05	9.0E+08	5.0E+07	3.0E+06	2.9E+06	8.0E+05	1.1E+09	7.0E+08
E	5.0E+08	8.0E+08	1.4E+09	9.0E+07	2.7E+06	3.0E+05	1.4E+09	9.0E+07	2.1E+06	2.4E+06	1.0E+06	1.2E+09	1.2E+09
Average (CFU/mL)	6.2E+08	5.6E+08	1.4E+09	1.1E+08	2.5E+06	2.7E+05	9.4E+08	7.6E+07	2.8E+06	2.8E+06	8.2E+05	1.2E+09	8.0E+08
Log Reduction													
A	-0.1619	0.7924	0.0731	1.3741	2.7051	3.7373	0.1280	1.0189	2.4546	2.4960	3.0700	0.0934	0.1392
B	0.1903	0.1903	-0.0782	1.1109	2.8513	3.7721	0.0700	1.1950	2.4818	2.5929	3.0700	-0.1370	0.3945
C	0.0934	-0.1619	0.2492	0.9762	2.7373	3.7051	0.0189	1.0189	2.5929	2.4546	3.1280	0.0142	0.2483
D	-0.1107	0.0142	-0.1487	1.0383	2.7373	3.6899	0.0189	1.2742	2.4960	2.5107	3.0700	0.0520	0.2483
E	0.0934	-0.1107	0.0062	1.1980	2.7209	3.6752	-0.1730	1.0189	2.6509	2.5929	2.9731	0.0142	0.0142
Average	0.0209	0.1449	0.0203	1.1395	2.7504	3.7159	0.0126	1.1052	2.5352	2.5294	3.0623	0.0074	0.2089
Error (+)	0.1694	0.6475	0.2289	0.2346	0.1009	0.0562	0.1155	0.1690	0.1157	0.0635	0.0658	0.0860	0.1855
Error (-)	0.1828	0.3067	0.1691	0.1633	0.0453	0.0407	0.1856	0.0863	0.0806	0.0748	0.0891	0.1444	0.1947

K12, log phase, LP	Test 5									
L (cm)	40.8									
1 (cm)	2.52									
a (1/cm)	0.062									
Petri Factor	0.98									
Reflection Factor	0.975									
Water Factor	0.8399									
Divergence Factor	0.9418									
E_o (mW/cm2) at 254nm	0.272									
E'_{avg} (mW/cm2)	0.2055									
UV Dose (mJ/cm^2)	0	15	15	20	2	10	10	2	5	5
Exposure time (h:m:s)		0:01:13	0:01:13	0:01:37	0:00:10	0:00:49	0:00:49	0:00:10	0:00:24	0:00:24
Colonies (per plate)										
A	9	34	14	17	4	4	4	11	19	25
B	10	23	18	22	1	5	7	4	23	15
C	5	29	15	19	9	4	9	2	25	16
D	15	30	24	21	9	9	3	7	18	22
E	8	30	19	18	10	5	6	5	17	24
Dilution factor	6	3	3	3	6	4	4	6	5	5
Volume plated (mL)	0.01	0.01	0.01	0.01	0.01	0.01	0.01	0.01	0.01	0.01
Colonies per mL										
A	9.0E+08	3.4E+06	1.4E+06	1.7E+06	4.0E+08	4.0E+06	4.0E+06	1.1E+09	1.9E+08	2.5E+08
B	1.0E+09	2.3E+06	1.8E+06	2.2E+06	1.0E+08	5.0E+06	7.0E+06	4.0E+08	2.3E+08	1.5E+08
C	5.0E+08	2.9E+06	1.5E+06	1.9E+06	9.0E+08	4.0E+06	9.0E+06	2.0E+08	2.5E+08	1.6E+08
D	1.5E+09	3.0E+06	2.4E+06	2.1E+06	9.0E+08	9.0E+06	3.0E+06	7.0E+08	1.8E+08	2.2E+08
E	8.0E+08	3.0E+06	1.9E+06	1.8E+06	1.0E+09	5.0E+06	6.0E+06	5.0E+08	1.7E+08	2.4E+08
Average (CFU/mL)	9.4E+08	2.9E+06	1.8E+06	1.9E+06	6.6E+08	5.4E+06	5.8E+06	5.8E+08	2.0E+08	2.0E+08
Log Reduction										
A	0.0189	2.4416	2.8270	2.7427	0.3711	2.3711	2.3711	-0.0683	0.6944	0.5752
B	-0.0269	2.6114	2.7179	2.6307	0.9731	2.2742	2.1280	0.3711	0.6114	0.7970
C	0.2742	2.5107	2.7970	2.6944	0.0189	2.3711	2.0189	0.6721	0.5752	0.7690
D	-0.2030	2.4960	2.5929	2.6509	0.0189	2.0189	2.4960	0.1280	0.7179	0.6307
E	0.0700	2.4960	2.6944	2.7179	-0.0269	2.2742	2.1950	0.2742	0.7427	0.5929
Average	0.0266	2.5112	2.7258	2.6873	0.2710	2.2619	2.2418	0.2754	0.6683	0.6730
Error (+)	0.2475	0.1002	0.1012	0.0554	0.7021	0.1092	0.2542	0.3967	0.0744	0.1241
Error (-)	0.2296	0.0695	0.1329	0.0566	0.2979	0.2430	0.2229	0.3437	0.0931	0.0978

Trials	Low Pressure												
			Logarithmic				Polynomial				Mamane-Linden			
Trial	Dose (mJ/cm^2)	Log Removal	ŷ	SS_R Values	Residual	Error	ŷ	SS_R Values	Residual	Error	ŷ	SS_R Values	Residual	Error
1	2	0.14	0.077136	2.80	0.0677	0.0046	0.115695	2.67	0.0292	0.0009	0.253650	2.24	-0.1088	0.0118
2	2	0.21	0.077136	2.80	0.1318	0.0174	0.115695	2.67	0.0932	0.0087	0.253650	2.24	-0.0448	0.0020
3	2	0.27	0.077136	2.80	0.1939	0.0376	0.115695	2.67	0.1553	0.0241	0.253650	2.24	0.0174	0.0003
4	2	0.28	0.077136	2.80	0.1983	0.0393	0.115695	2.67	0.1597	0.0255	0.253650	2.24	0.0218	0.0005
5	5	1.14	1.289277	0.21	-0.1498	0.0224	1.114986	0.40	0.0245	0.0006	0.995533	0.57	0.1440	0.0207
6	5	1.11	1.289277	0.21	-0.1841	0.0339	1.114986	0.40	-0.0098	0.0001	0.995533	0.57	0.1096	0.0120
7	5	0.67	1.289277	0.21	-0.6210	0.3856	1.114986	0.40	-0.4467	0.1995	0.995533	0.57	-0.3272	0.1071
8	5	0.67	1.289277	0.21	-0.6163	0.3798	1.114986	0.40	-0.4420	0.1954	0.995533	0.57	-0.3226	0.1041
9	10	2.75	2.206226	0.21	0.5442	0.2961	2.303619	0.31	0.4468	0.1996	2.158837	0.17	0.5915	0.3499
10	10	2.54	2.206226	0.21	0.3290	0.1083	2.303619	0.31	0.2316	0.0536	2.158837	0.17	0.3764	0.1417
11	10	2.26	2.206226	0.21	0.0557	0.0031	2.303619	0.31	-0.0417	0.0017	2.158837	0.17	0.1031	0.0106
12	10	2.24	2.206226	0.21	0.0356	0.0013	2.303619	0.31	-0.0618	0.0038	2.158837	0.17	0.0830	0.0069
13	15	3.72	2.742607	0.98	0.9733	0.9473	2.896187	1.31	0.8197	0.6720	2.722617	0.95	0.9933	0.9867
14	15	2.53	2.742607	0.98	-0.2132	0.0454	2.896187	1.31	-0.3668	0.1345	2.722617	0.95	-0.1932	0.0373
15	15	2.51	2.742607	0.98	-0.2315	0.0536	2.896187	1.31	-0.3850	0.1483	2.722617	0.95	-0.2115	0.0447
16	15	2.73	2.742607	0.98	-0.0168	0.0003	2.896187	1.31	-0.1703	0.0290	2.722617	0.95	0.0032	0.0000
17	20	3.06	3.123175	1.88	-0.0610	0.0037	2.892691	1.30	0.1695	0.0287	3.001497	1.57	0.0607	0.0037
18	20	2.69	3.123175	1.88	-0.4359	0.1900	2.892691	1.30	-0.2054	0.0422	3.001497	1.57	-0.3142	0.0987

K12, LP, Regression Models					
Coefficients to Different Trendlines					
Logarithmic		Polynomial 2nd Order		Mamane-Linden Coefficients	
β_0	-0.83981228	β_0	-0.66971123	k1	0.2810
β_1	1.322877743	β_1	0.41654599	k2	0.0490
		β_2	-0.01192129	d	0.4030
				a	0.0096

Analysis of Regression									
Type	Sum of Squares	Degrees of Freedom	Mean Square (MS_R)	Sum of Errors SS_E	Degrees of Freedom	Mean Square (MS_E)	Fo	pvalue	R^2
Log	20.59	1	20.58781	2.5697	16	0.160604	128.1899	4.755E-09	0.88903
Polynomial	21.29	2	10.69461	1.7683	15	0.117884	90.72185	4.182E-09	0.92364
Mamane	18.82	1	18.81894	1.9387	16	0.121168	155.3123	1.187E-09	0.90660

Trials	LED													
			Logarithmic				Polynomial				Mamane-Linden			
Trial	Dose (mJ/cm²)	Log Removal	ŷ	SS_E Values	Residual	Error	ŷ	SS_E Values	Residual	Error	ŷ	SS_E Values	Residual	Error
1	1.50	0.22	0.070586552	4.40	0.1449	0.0210	0.557348754	2.60	-0.3418	0.1169	0.438357966	3.00	-0.2229	0.0497
2	2.00	0.50	0.448797464	2.96	0.0506	0.0026	0.690411348	2.19	-0.1910	0.0365	0.577908701	2.53	-0.0785	0.0062
3	2.00	0.45	0.448797464	2.96	-0.0032	0.0000	0.690411348	2.19	-0.2448	0.0599	0.577908701	2.53	-0.1323	0.0175
4	2.20	0.37	0.574100198	2.54	-0.2029	0.0412	0.742846245	2.03	-0.3717	0.1381	0.633216579	2.36	-0.2620	0.0687
5	3.60	0.66	1.221550973	0.90	-0.5634	0.3175	1.09724827	1.15	-0.4391	0.1928	1.011487697	1.34	-0.3534	0.1249
6	3.70	1.33	1.257571956	0.83	0.0773	0.0060	1.121716121	1.10	0.2132	0.0454	1.037828851	1.28	0.2971	0.0882
7	3.70	1.28	1.257571956	0.83	0.0196	0.0004	1.121716121	1.10	0.1554	0.0242	1.037828851	1.28	0.2393	0.0573
8	5.00	1.61	1.653429893	0.27	-0.0385	0.0015	1.429526351	0.55	0.1854	0.0344	1.369555075	0.64	0.2453	0.0602
9	5.00	1.70	1.653429893	0.27	0.0456	0.0021	1.429526351	0.55	0.2695	0.0726	1.369555075	0.64	0.3295	0.1086
10	7.20	2.47	2.132820227	0.00	0.3359	0.1128	1.906978228	0.07	0.5617	0.3155	1.868672234	0.09	0.6000	0.3600
11	7.30	3.13	2.150954082	0.00	0.9822	0.9646	1.927382498	0.06	1.2057	1.4538	1.889023168	0.08	1.2441	1.5478
12	10.00	2.15	2.564699148	0.16	-0.4166	0.1736	2.435630171	0.07	-0.2875	0.0827	2.354251329	0.03	-0.2062	0.0425
13	10.00	2.57	2.564699148	0.16	0.0013	0.0000	2.435630171	0.07	0.1303	0.0170	2.354251329	0.03	0.2117	0.0448
14	10.80	2.98	2.665878569	0.25	0.3123	0.0975	2.570419258	0.16	0.4078	0.1663	2.463910263	0.09	0.5143	0.2645
15	10.90	2.76	2.677995554	0.26	0.0823	0.0068	2.586759946	0.17	0.1735	0.0301	2.476886286	0.09	0.2834	0.0803
16	14.50	2.62	3.053187674	0.78	-0.4291	0.1841	3.099848466	0.87	-0.4757	0.2263	2.872765944	0.50	-0.2487	0.0618
17	15.00	3.75	3.097757489	0.86	0.6506	0.4233	3.159540842	0.98	0.5888	0.3467	2.92101032	0.57	0.8273	0.6845
18	15.00	2.18	3.097757489	0.86	-0.9202	0.8467	3.159540842	0.98	-0.9820	0.9642	2.92101032	0.57	-0.7434	0.5527
19	15.00	2.47	3.097757489	0.86	-0.6239	0.3892	3.159540842	0.98	-0.6857	0.4702	2.92101032	0.57	-0.4472	0.1999
20	20.00	4.17	3.475968402	1.71	0.6938	0.4813	3.601258363	2.05	0.5685	0.3232	3.376161111	1.46	0.7936	0.6298
21	20.00	3.43	3.475968402	1.71	-0.0462	0.0021	3.601258363	2.05	-0.1715	0.0294	3.376161111	1.46	0.0536	0.0029
22	20.00	2.71	3.475968402	1.71	-0.7629	0.5820	3.601258363	2.05	-0.8882	0.7889	3.376161111	1.46	-0.6631	0.4397
23	25.00	4.38	3.769331577	2.56	0.6106	0.3729	3.760782736	2.53	0.6192	0.3834	3.817723586	2.72	0.5623	0.3161

K12, LP, Regression Models					
Coefficients to Different Trendlines					
Logarithmic		Polynomial 2nd Order		Mamane-Linden Coefficients	
β_0	-0.46247179	β_0	0.14122938	k1	0.2870
β_1	1.314683634	β_1	0.28587871	k2	0.0880
		β_2	-0.00564386	d	-0.0240
				a	0.0247

Analysis of Regression									
Type	Sum of Squares	Degrees of Freedom	Mean Square (MS_E)	Sum of Errors SS_E	Degrees of Freedom	Mean Square (MS_E)	Fo	pvalue	R^2
Log	27.83	1	27.83180	5.0292	21	0.239487	116.2141	5.12E-10	0.84695
Polynomial	26.54	2	13.27121	6.3186	20	0.315931	42.00672	6.91E-08	0.80772
Mamane	25.29	1	25.29478	5.8086	21	0.276598	91.44957	4.21E-09	0.81325

Trials	Low Pressure													
			Logarithmic				Polynomial				Mamane			
Trial	Dose (mJ/cm²)	Log Removal	ŷ	SS_R Values	Residual	Error	ŷ	SS_R Values	Residual	Error	ŷ	SS_R Values	Residual	Error
1	2	0.23	0.09864012	3.11	0.1264	0.0160	0.114901806	3.06	0.1101	0.0121	0.253650435	2.59	-0.0286	0.0008
2	5	0.90	1.27975400	0.34	-0.3833	0.1469	1.115863984	0.56	-0.2194	0.0481	0.995533906	0.75	-0.0990	0.0098
3	10	2.45	2.17323217	0.10	0.2741	0.0751	2.304701596	0.20	0.1426	0.0203	2.158837502	0.09	0.2885	0.0832
4	15	2.87	2.69588338	0.69	0.1747	0.0305	2.894248355	1.06	-0.0237	0.0006	2.722617204	0.74	0.1480	0.0219
5	20	2.87	3.06671033	1.45	-0.1919	0.0368	2.884504259	1.04	-0.0097	0.0001	3.001497426	1.30	-0.1267	0.0161

K12, LP, Regression Models					
Coefficients to Different Trendlines					
Logarithmic		Polynomial 2nd Order		Mamane-Linden Coefficients	
β_0	-0.79483804	β_0	-0.6722645	k1	0.2810
β_1	1.289016511	β_1	0.4175548	k2	0.0490
		β_2	-0.0119858	d	0.4030
				a	0.0096

Analysis of Regression									
Type	Sum of Squares	Degrees of Freedom	Mean Square (MS_R)	Sum of Errors SS_E	Degrees of Freedom	Mean Square (MS_E)	Fo	pvalue	R^2
Log	5.69	1	5.691999	0.3054	3	0.101787	55.92080	0.004953	0.94908
Polynomial	5.92	2	2.958052	0.0813	2	0.040628	72.80877	0.013549	0.98645
Mamane	5.47	1	5.465084	0.1318	3	0.043936	124.3870	0.001545	0.97645

Trials	LED													
			Logarithmic				Polynomial				Mamane			
Trial	Dose (mJ/cm^2)	Log Removal	ŷ	SS_E Values	Residual	Error	ŷ	SS_E Values	Residual	Error	ŷ	SS_E Values	Residual	Error
1	2.00	0.44	0.512575374	2.78	-0.0739	0.0055	0.654517749	2.33	-0.2158	0.0466	0.577908701	2.57	-0.1392	0.0194
2	3.60	1.09	1.265532303	0.84	-0.1755	0.0308	1.166797479	1.03	-0.0767	0.0059	1.011487697	1.37	0.0786	0.0062
3	5.00	1.66	1.686347248	0.24	-0.0294	0.0009	1.56974447	0.37	0.0872	0.0076	1.369555075	0.66	0.2874	0.0826
4	7.30	2.80	2.171125745	0.00	0.6298	0.3966	2.139946898	0.00	0.6610	0.4369	1.889023168	0.09	0.9119	0.8315
5	10.00	2.36	2.574271393	0.15	-0.2172	0.0472	2.663714984	0.23	-0.3067	0.0940	2.354251329	0.03	0.0028	0.0000
6	10.90	2.87	2.684665346	0.25	0.1846	0.0341	2.80336035	0.39	0.0659	0.0043	2.476886286	0.09	0.3923	0.1539
7	15.00	2.80	3.093673721	0.83	-0.2937	0.0863	3.218426305	1.08	-0.4185	0.1751	2.92101032	0.55	-0.1211	0.0147
8	20.00	3.44	3.462195538	1.64	-0.0247	0.0006	3.233878433	1.11	0.2036	0.0415	3.376161111	1.43	0.0614	0.0038

K12, LP, Regression Models					
Coefficients to Different Trendlines					
Logarithmic		Polynomial 2nd Order		Mamane-Linden Coefficients	
β_0	-0.79483804	β_0	-0.6722645	k1	0.2810
β_1	1.289016511	β_1	0.4175548	k2	0.0490
		β_2	-0.0119858	d	0.4030
				a	0.0096

Analysis of Regression									
Type	Sum of Squares	Degrees of Freedom	Mean Square (MS_E)	Sum of Errors SS_E	Degrees of Freedom	Mean Square (MS_E)	Fo	pvalue	R^2
Log	5.69	1	5.691999	0.3054	3	0.101787	55.92080	0.004953	0.94908
Polynomial	5.92	2	2.958052	0.0813	2	0.040628	72.80877	0.013549	0.98645
Mamane	5.47	1	5.465084	0.1318	3	0.043936	124.3870	0.001545	0.97645